D6.3 Model calibration and parametric study

Report To RFCS, as a deliverable from the research project:

Execution and reliability of slip resistant connections for steel structures using carbon steel and stainless steel (SIROCO)

Document: RT1763
Version: 03
Date: 19 March 2018

SCI, Silwood Park, Ascot,
Berkshire, UK, SL5 7QN
Tel: + 44(0) 1344 636525
Fax: + 44(0) 1344 636570

Version	Issue	Purpose	Author	Reviewer	Approved
01	01	First draft for internal review	AQC	NRB	
02	01	For comment by partners	AQC	NRB	NRB
03	01	Final version	AQC	NRB	NRB

For information on publications, telephone direct: +44 (0) 1344 636505
or Email: publications@steel-sci.com

For information on courses, telephone direct: +44 (0) 1344 636500
or Email: education@steel-sci.com

Email: reception@steel-sci.com

World Wide Web site: http://www.steel-sci.org

EXECUTIVE SUMMARY

This document is D6.3 *Report on the parametric study*, a deliverable of the RFCS project *Execution and reliability of slip resistant connections for steel structures using Carbon Steel and Stainless Steel* (SIROCO), Grant Agreement number RFSR-CT-2014-00024.

Stainless steel is often selected for structures in corrosive environments, or where the architectural design requires an alternative design solution to carbon steel for aesthetic purposes. Slip resistant connections are required for a range of structures such as bridges, cranes, radio masts, wind turbines etc., where slip has to be restricted and/or the structure is subject to fluctuating load. Design and execution rules for carbon steel slip resistant connections are given EN 1993-1-8 and EN 1090-2. However, comparable rules for stainless steel applications do not exist.

The SIROCO project studied the visco-plastic behaviour of stainless steel bolts, plates and bolted assemblies. Furthermore, preloading behaviour of stainless steel bolted assemblies and the performance of stainless steel slip resistant connections were investigated. Numerical studies were conducted to generate additional data on the slip resistant behaviour of stainless steel connections. Design rules were developed based on the test and numerical investigations.

The numerical model developed previously was extended with a surface friction model and calibrated against slip factor tests of stainless steel preloaded bolted connections. The slip response and long term behaviour of the numerical models have been also evaluated by comparing against relaxation and extended creep tests of bolted assemblies. It was shown that the numerical model is able to accurately predict both short and long term behaviour of stainless steel slip resistant connections.

The parametric study showed that the plate thickness to bolt diameter ratio should be between 2-4 for better slip resistance. It was also observed that the bolt size does not affect the slip resistance of the connection.

The numerical studies confirmed the experimental findings that the visco-plastic behaviour of stainless steel has been overstated in the past. The loss of preload in preloaded stainless steel bolts is not excessive and the slip resistance performance in the long term is not affected by the visco-plastic deformation of stainless steel.

Contents

1 INTRODUCTION

The usage of stainless steel can lead to significant reduction in maintenance costs compared to structures constructed using carbon steel. Stainless steel is becoming more popular as a building material because of its high material strength, ductility and corrosion resistance. However, there are no design rules for stainless steel preloaded bolts, partly due to concerns about its visco-plastic behaviour and a lack of knowledge about how creep and stress relaxation at room temperature would affect performance. In the frame of the European RFCS research project Execution and reliability of slip resistant connections for steel structures using Carbon Steel and Stainless Steel (SIROCO), slip factors for difference stainless steel grades were determined [1,2] by experiments according to EN 1090-2 Annex G [3] to investigate the effects of time dependant material behaviour. Extensive studies [4,5] were also carried out on the tightening and preloading behaviour of EN ISO 4014 [6] and 4017 [7] bolting systems made of austenitic and duplex stainless steels.

Advanced non-linear FE models of stainless steel bolting assemblies and slip-resistant connections based on the specification in EN1090-2 Annex G have been developed and validated in WP5 of the SIROCO project [8,9]. The numerical models focused on the time-dependent material model of stainless steel bolts and plates. Preliminary model calibrations have been conducted to show the validity of the numerical model in predicting the slip behaviour of preloaded stainless steel connections in Task 5.5.

The main objectives of Task 6.4 (reported in this Deliverable 6.3) are:

(1) to extend the model developed in Task 5.5 and calibrate it against the extensive test programme of preloaded stainless steel connections in WP6, and

(2) to study a large number of additional cases with different geometric or material parameters.

The influence of the visco-plastic characteristics of stainless steel on the slip behaviour of preloaded bolted connection have been examined in detail using these numerical models. Both the tests and these numerical results were used to develop design recommendations for slip-resistant stainless steel connections, which are reported in Deliverable 6.4.

2 CALIBRATION AND EVALUATION OF NUMERICAL MODELS

Two types of numerical model have been developed in the SIROCO project:

(1) 2D axisymmetric model for studying the stainless steel bolt preload, and

(2) 3D double symmetric model for investigating the slip behaviour of preloaded stainless steel connections.

This chapter presents the calibration of the numerical models using tests results available from the project and the evaluation of the numerical models in predicting the long term behaviour of stainless steel slip resistant connections and preloaded bolt assemblies.

2.1 Numerical models of slip-resistant connections

Details of the development of the numerical models are presented in the deliverable D5.6 [9] of the SIROCO project. Key aspects of the models are described in the following sections where new analysis and discussion are presented.

2.1.1 2D axisymmetric model – single bolt assembly

The 2D axisymmetric model, as shown in Figure 2.1, has been developed to study the preload relaxation of a stainless steel bolted connection. This model offers an efficient way to investigate the time-dependent behaviour of stainless steel in a preloaded bolt assembly and validate the visco-plastic material model proposed in WP 5 [10,11].

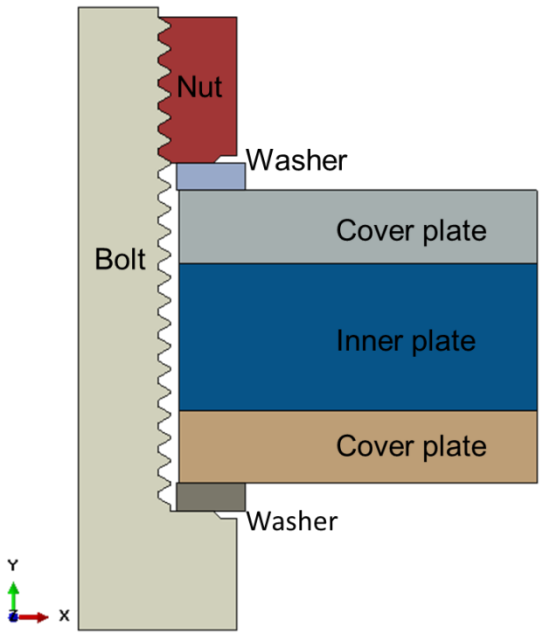

Figure 2.1 2D axisymmetric model for study of bolt preload

2.1.2 3D double symmetric model – slip factor test

In the frame of the SIROCO project, slip factor tests were carried out to determine slip factors for different grade of stainless steel with typical surface finishes [1, 2]. Four grades of stainless steel were tested: austenitic (1.4404), duplex (1.4462), lean-duplex (1.4162) and ferritic (1.4003). The austenitic stainless steel bolts used in the test are produced by BUMAX (BUMAX 88 and 109).

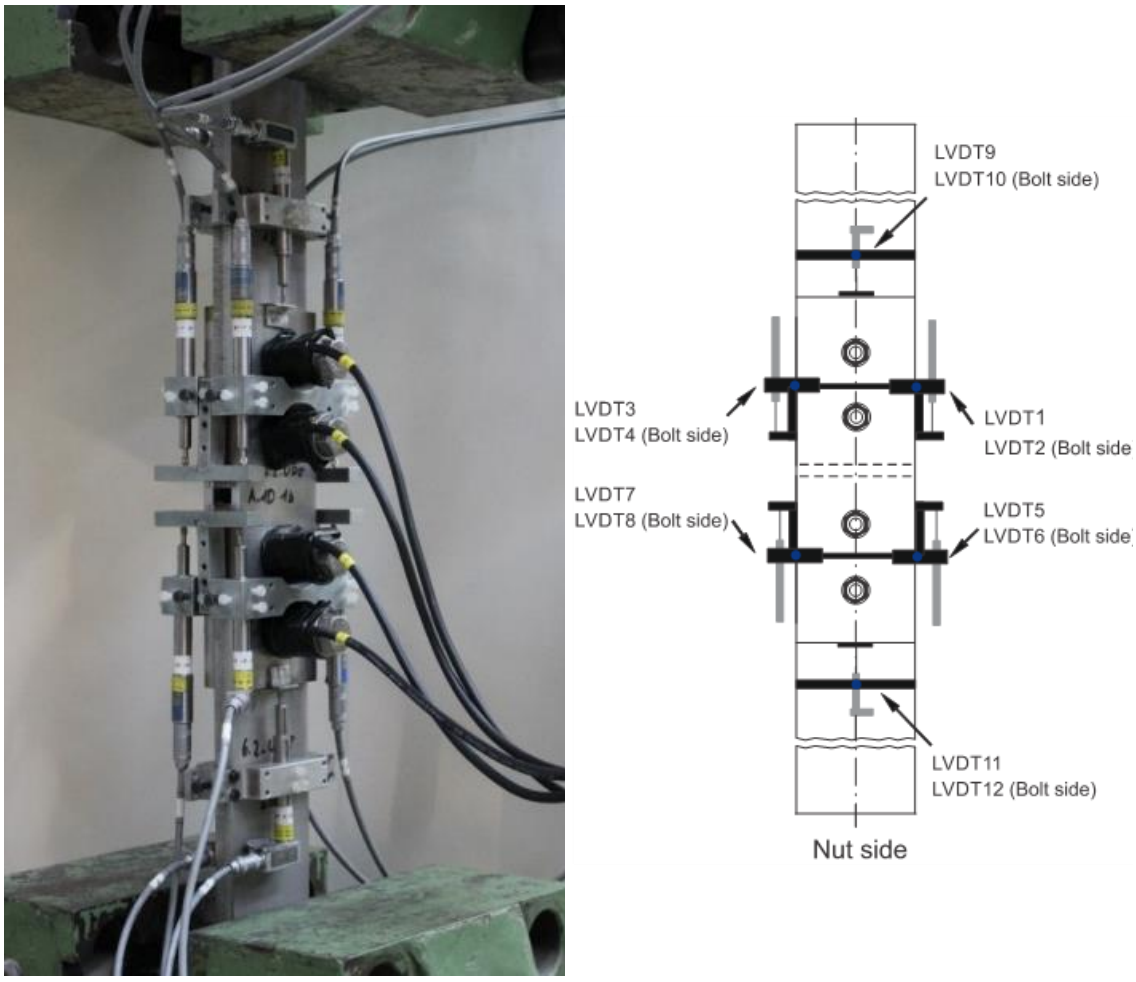

(a) Test set-up

(b) Schematics of displacement measurement

Figure 2.2 Slip factor test configuration according to EN1090-2, Annex G (© UDE)

The test set-up according to EN 1090-2 Annex G [12] to determine slip factor is shown in Figure 2.2. Specially made load cells were used in the tests to monitor the preload in the bolts. As a result, the clamping length of the specimen assembly was slightly longer than the specification from Annex G EN 1090-2. Linear variable displacement transformers (LVDT), as shown in Figure 2.2, were used in the tests to record the slip between the clamped plates when the shear force was applied. LVDT1-8 were used to measure the slip occurring between the central bolt groups (CBG) while LVDT9-12 were placed away from the centre to measure the slip occurring at the plate end (PE).

The grades and sizes of the stainless steel components used in the tests were limited in order to contain costs. Advanced finite element (FE) models were therefore developed in ABAQUS to extend the scope of the study [8, 9], so that the behaviour of the stainless steel slip resistant connections of different size and material type can be examined.

The 3D FE model of the slip test specimen is shown in Figure 2.3. Only one quarter of the full size assembly is created to take advantage of symmetry and improve the efficiency. The bolt preload is applied by shortening the bolt shank length and the UAMP subroutine is used to monitor the bolt load and start the slip test step once the desired preload is reached.

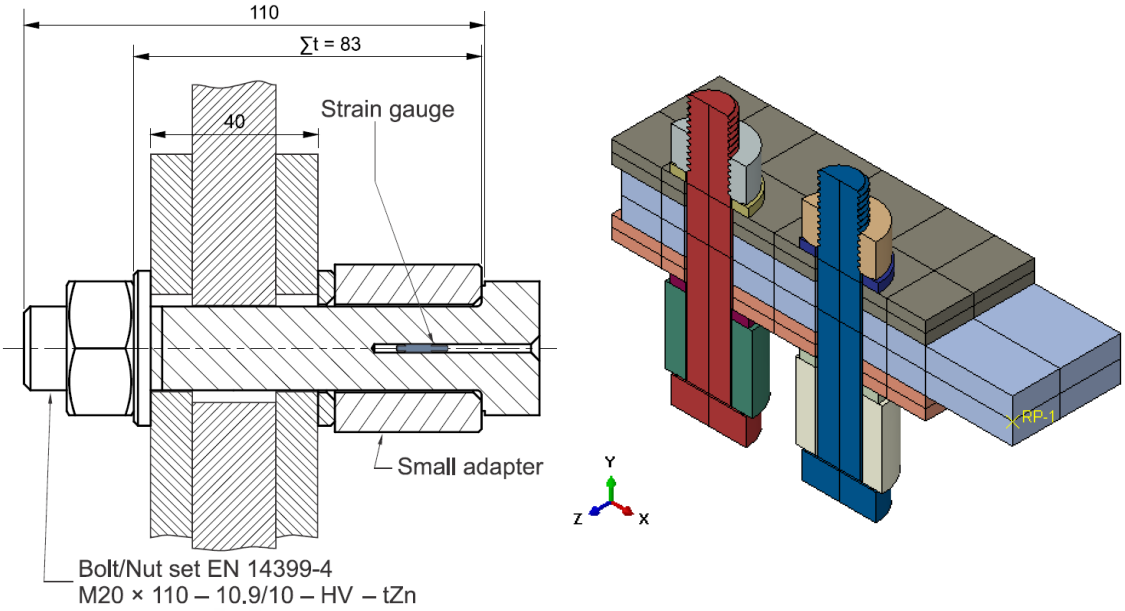

(a) Technical drawing (© UDE) (b) FE model of slip factor test

Figure 2.3 3D double symmetric model (according to EN1090-2 Annex G)

The visco-plastic material model (Chaboche model) was used to model various grades of stainless steel plates and bolts used in the tests. Plate and bar materials were tested and the Chaboche model was fitted against the results [10, 11]. The calibrated material model and parameters are presented in Section 2.4.

2.2 Preliminary calibration against tests on carbon steel connections

The validation of the FE model presented in the previous section involves: (1) validation of the visco-plastic material behaviour of the stainless steel material in the preloaded bolt assembly and (2) calibration of the static coefficient of friction between the faying surfaces of the plates.

Prior to the tests on the stainless steel plates and bolts, slip factor tests were carried out using carbon steel connections. M20 grade 10.9 bolts were used and the dimensions of the components were defined according to EN 1090 Part 2 Annex G [3]. The test results were used in a preliminary numerical study in which the friction coefficient of grit blasted carbon steel plates was calibrated and the behaviour of the assembly during the test was examined.

Adaptors of different length were used to study the effect of clamping length on the response of the connection. The elasto-perfect-plastic material model was used for carbon steel material in the test. The Young's modulus and yield stress assumed for each component are presented in Table 2.1.

Table 2.1 Material properties of slip-resistant carbon steel connection

	Bolt	Nut	Plate/Adaptor	Washer
σ_y (MPa)	918	1020	362.1	979.2
E	210 GPa			

In this preliminary validation work of the carbon steel connection, the value of the friction coefficient μ_{fric} was determined so that the nominal slip factor is the same as that measured in the test. Figure 2.4 presents the calibration of the static coefficient of friction against the test results of the connection with a clamping length of 52 mm. It was found that by assuming μ_{fric} = 0.817 in the FE model, the slip factor would be the same as the test.

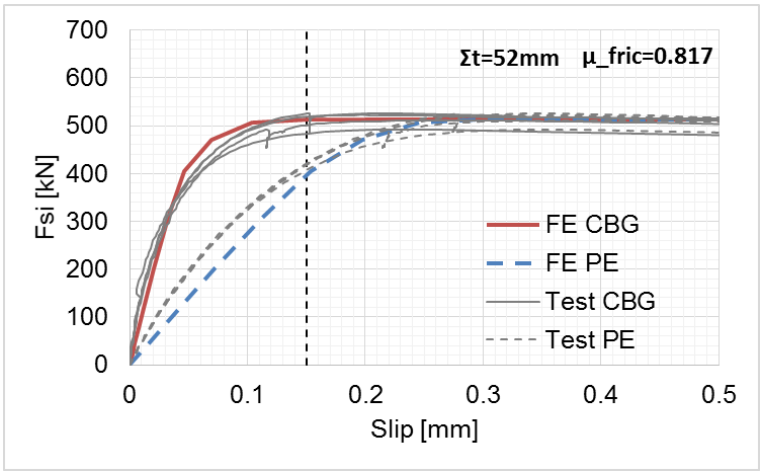

Figure 2.4 Comparison of slip behaviour of the numerical model against test results and calibration of the static coefficient of friction

The numerical slip load – displacement curves are compared with the test data in Figure 2.4. It can be seen that the FE model is in good agreement with the test results. The slip behaviour at both CBG and PE positions were successfully reproduced by the numerical model. The comparison of slip factors at different clamping length is shown in Figure 2.5. The numerical model suggested that longer clamping lengths lead to higher slip factors which is consistent with the test results.

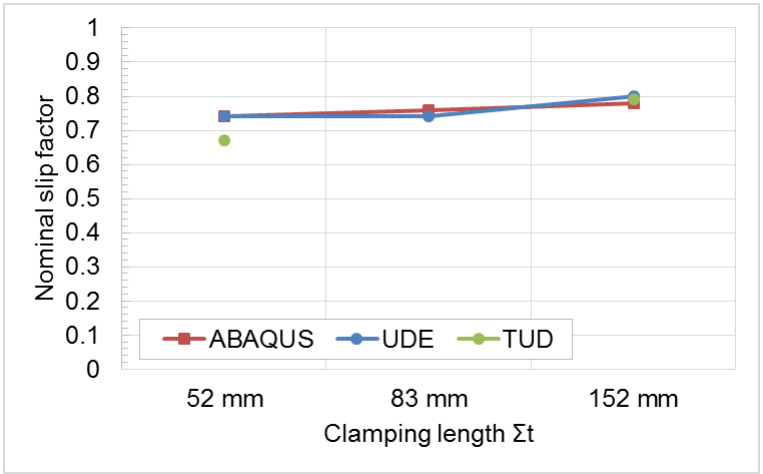

Figure 2.5 Effect of clamping length on the nominal slip factor of carbon steel slip resistant connection

Figure 2.6 compares the high contact pressure areas in the FE model with the actual observation made after the slip test. Figure 2.6(a) shows the contact pressure before and after the slip test over the faying surface of the inner plate. Figure 2.6(b) shows the contact pressure over the faying surface of the cover plate. The area of the FE model under high contact stress is very similar to the area of the surface damage due to high compressive pressure found in the test as shown in Figure 2.6(c).

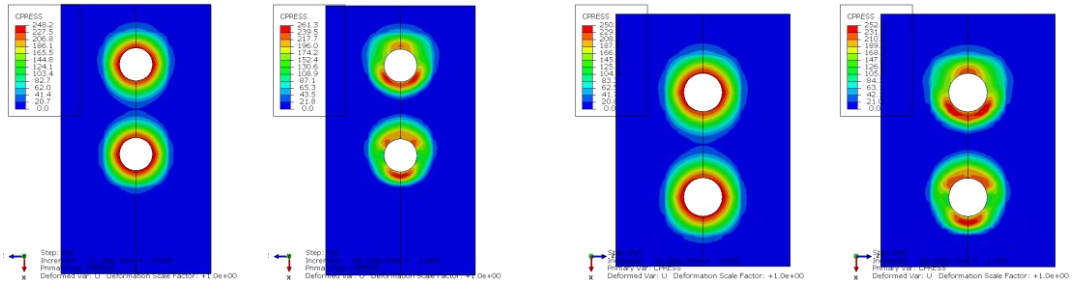

(a) Faying surface of Inner plate (b) Faying surface of cover plate

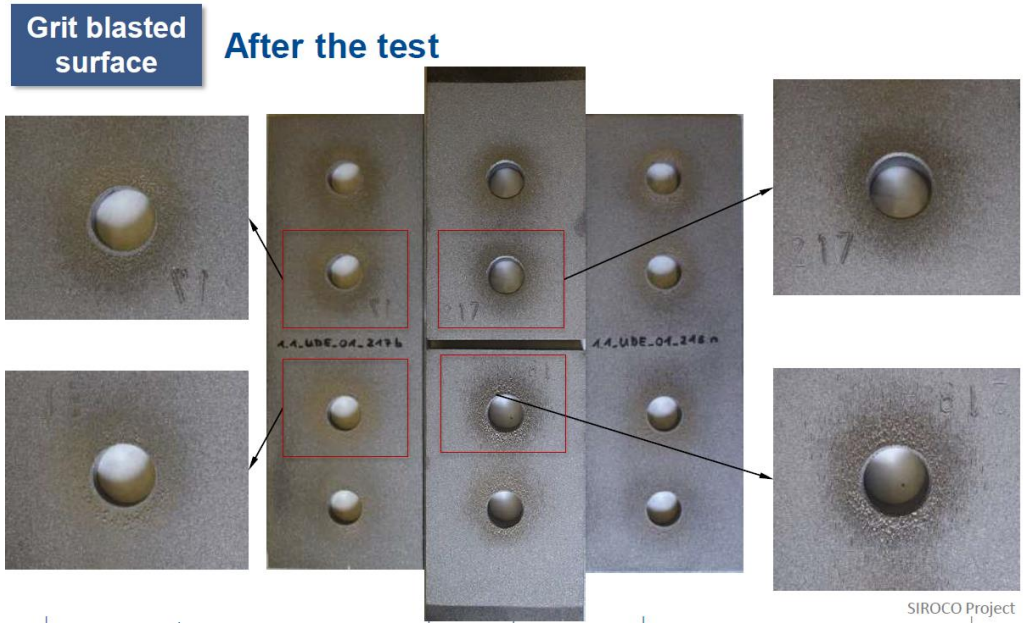

(c) Actual damage to the faying surface after test (© UDE)

Figure 2.6 (a) & (b) – pressure distribution over the faying surface between cover plate and inner plate (left: under preload, right: after slip test); (c) – actual damage of the faying surface after test

The surface damage observed after testing suggested that the high spots on these roughened surfaces were probably due to yielding in compression. It is possible that, at these pressure levels, friction is not independent of normal contact pressure. This might explain the coefficient of friction used in the numerical model (μ_{fric} = 0.817) is greater than the widely reported value of 0.48 – 0.55 for a grit blasted surface finish.

2.3 Estimation of loss of preload

In slip resistant connections, there will often be some loss of tension in individual bolts after they are pre-tensioned. Two major sources of loss of bolt preload are setting (surface embedment) and contraction of plates under shear force.

The surface of the components in a bolted assembly (threads in the nut and bolt, washers, faying surfaces of the plates) are full of asperities, especially when the plate surfaces are treated for better frictional performance. When these parts are loaded under compression by the bolt preload, they contact each other only at the high spots over a relatively small contact area. The resulting high compressive pressure would cause plastic deformation of the metal spikes on the surface. This embedment or setting effect would lead to some loss of preload in the bolts. When the slip resistant connection is subject to shear load, the contraction of the plate will lead to further loss of the preload in the bolts.

The loss of preload due to embedment and plate contraction can be estimated by using German design guidance VDI 2230 Part 1 [13].In the frame of the preliminary study, the loss of preload in class 10.9 M20 bolts with different clamping lengths were examined. The required geometry and material parameters for the hand calculation are tabulated in Table 2.2.

Table 2.2 Geometry and material for preload loss calculation (slip-resistant carbon steel connection with grit blasted surface finish and class 10.9 M20 bolts, clamping length Σt=83mm)

l_k [1]	83 mm	l_1 [2]	83 mm	l_{GEW} [3]	0 mm
D_w [4]	29.5 mm	D_h [5]	22 mm	d [6]	20 mm
d_3 [7]	17.29 mm	D_A [8]	36 mm	A_N [9]	314.2 mm^2
A_{d3} [10]	234.8 mm^2	E_s [11]	210000 MPa	E_M [12]	210000 MPA
E_p [13]	210000 MPa	w [14]	1	b [15]	100 mm
t [16]	20 mm	n [17]	2	m [18]	2
μ [19]	0.74	$F_{p,c}$ [20]	172 kN		

[1] total clamping length | [2] length of unthreaded bolt shank | [3] length of unengaged thread part of the bolt | [4] effective head diameter | [5] hole diameter | [6] bolt major diameter | [7] bolt minor diameter | [8] effective diameter of the compressive cone | [9] major area of the bolt | [10] minor area of the bolt | [11],[12],[13] Young's modulus of bolt, nut and plates | [14] constant w=1 for through bolted joint | [15] inner plate width | [16] inner plate thickness | [17] number of bolts | [18] number of plates | [19] slip factor | [20] bolt preload

The calculation procedure and details are presented in Appendix A. According to VDI 2231-1, the total resilience (δ) of bolt (δ_s) and clamped plate (δ_p) are obtained as:

$$\delta = \delta_s + \delta_p = 1.73 \times 10^{-6} + 6.72 \times 10^{-7} = 2.406 \times 10^{-6}\, mm/N$$

The transverse contraction is determined as $f_y = 14.55\, \mu m$ and the setting on all the contact surface pairs is estimated as $f_z = 3 + 2.5 + 3.5 + 3.5 + 2.5 + 3 + 3 = 21\, \mu m$.

The loss of preload due to transverse contraction and setting therefore is:

$$\Delta F_{p,c,contraction} = \frac{f_y}{\delta_s + \delta_p} = \frac{14.55}{2.406} = 6.05\, kN \;\rightarrow LP = \frac{3.97}{172} = 3.5\%$$

$$\Delta F_{p,c,setting} = \frac{f_z}{\delta_s + \delta_p} = \frac{21}{2.406} = 8.73\ kN \rightarrow LP = \frac{6.05}{172} = 5.1\%$$

The preload loss predicted by VDI guidance and the FE model are compared with the test measurement in Figure 2.7. It can be seen that for the three clamping lengths examined here, the predicted total loss of preload by FE models and hand calculation are in reasonably good agreement with the test results. The loss of preload was reduced when a longer clamping length was used. This effect was captured well by both prediction tools.

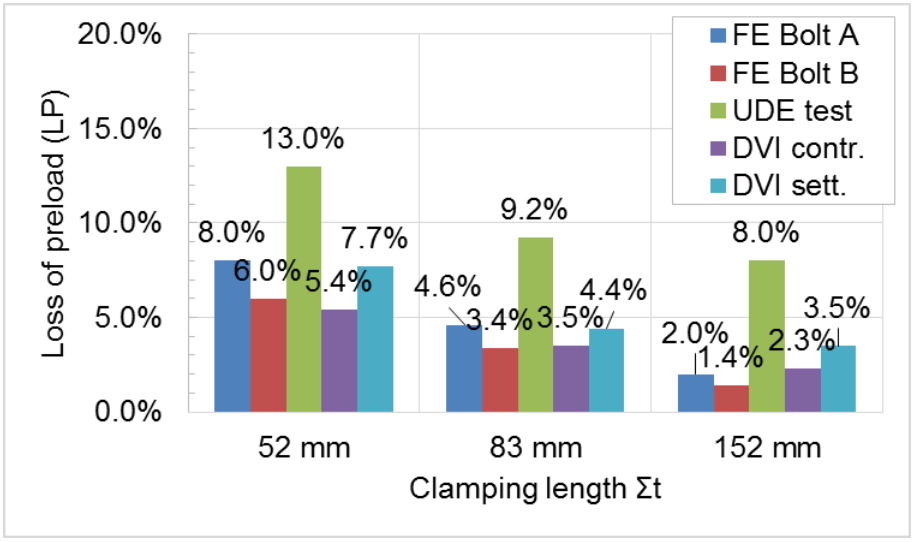

Figure 2.7 Influence of clamping length on loss of preload during slip test

2.4 Material models of stainless steel

The stainless steel material models used in the current work package were developed and calibrated in the previous work package [4, 10, 11], where extensive studies were carried out to test the strength and to investigate the relaxation behaviour of the stainless steel plate and bolt material. The material data on strength and relaxation behaviour were used subsequently to calibrate the visco-plastic and creep model to be used in the numerical investigation. The material models and parameters are summarised in the following section.

2.4.1 Stainless steel plate

The stainless steel plate material is modelled using the Chaboche model (a visco-plastic model, implemented in ABAQUS by subroutine UHARD). The constitutive equation and parameters to be identified are shown in Equation (1). The model parameters for four grades of stainless steel plates were identified in Task 5.2 [10]. The Subroutine UHARD was developed and tested in Task 5.2 as well.

$$\sigma = k + Q\left(1 - e^{-b\bar{\epsilon}_p}\right) + \sum_{i=1}^{3} \frac{C_i}{\gamma_i}\left(1 - e^{-\gamma_i \bar{\epsilon}_p}\right) + D\left(\dot{\bar{\epsilon}}_p\right)^{\frac{1}{n}} \quad (1)$$

Where

σ = stress

$\bar{\epsilon}_p$ = plastic strain

$\dot{\bar{\epsilon}}_p$ = plastic strain rate

k, Q, b = parameters to be identified for the isotropic strain hardening model

C_i, γ_i = parameters to be identified for the kinematic strain hardening model

D, n = parameters to be identified for the strain rate hardening model

The parameters of the visco-plastic model for stainless steel plates used in the project are shown in Table 2.3.

Table 2.3 Unified Chaboche model parameters for stainless steel plate

Grade	D [MPa]	n[-]	C_1 [MPa]	γ_1 [-]	C_2 [MPa]	γ_2 [-]	C_3 [MPa]	γ_3 [-]	Q [MPa]	b [-]	k [MPa]
Austenitic 1.4404	110	15.0	45949	591.4	617031	6765.3	1434	2.5	380	2.5	73
Ferritic 1.4003	130	11.0	623733	5855.1	17430	558.6	1680	10.8	104	10.8	106
Duplex 1.4462	313	24.3	947349	11334.6	252038	1222.1	2971	60.0	723	2.8	106
Lean duplex 1.4162	329	30.2	483769	4875.7	102445	975.3	6766	180.8	649	3.5	109

2.4.2 Stainless steel bolt

The study of material strength and visco-plastic behaviour of stainless steel bolts was carried out in Task 5.3 [11]. Two types of material model were proposed for the bolt material and they are summarised below.

CREEP subroutine and calibrated parameters for stainless steel bolt

The stress relaxation behaviour of various types stainless steel bolt materials were available from Task 5.2 [8]. In order to use the results from the stress relaxation test in the FE model to simulate the creep and relaxation behaviour of the stainless steel bolts, a strain-hardening creep model was developed by VTT [8] and it is shown in the Equation (2) below.

$$\dot{\varepsilon_v} = c\left[\frac{\varepsilon_v(1-b)}{c} + a^{1-b}\right]^{\frac{b}{b-1}} \quad (2)$$

Where

$\dot{\varepsilon_v}$ = creep strain rate

ε_v = creep strain

The strain-hardening model is used to reproduce the relaxation curve at any preloading level used in the stress relaxation test. The parameter c can be calibrated as a variable dependent on the initial stress σ_0 in the relaxation test according to Equation (3).

$$c = c_1\sigma_0^2 + c_2\sigma_0 + c_3 \quad (3)$$

Where c_1, c_2 and c_3 are constants fitted to stress relaxation test results.

A simpler linear fit can also be used for the c parameter as shown in the Equation (4).

$$c = c_4\sigma_0 + c_5 \quad (4)$$

The curve fitting of the stress relaxation test results was carried out by VTT. The model was fitted to experiments of austenitic, duplex and lean duplex bolt bar material. The parameter sets are shown in Table 2.4 and Table 2.5.

Table 2.4 Parameters of strain hardening model of cold-drawn bars with parabolic approximation of coefficient c

Grade	a	b	c_1 x 10^{10}	c_2 x 10^8	c_3 x 10^5
Austenitic 1.4401	0.5229	1.0371	1.0011	-6.1588	1.7196
Lean duplex 1.4162	0.6010	1.0537	1.2623	-7.5340	2.0036
Duplex 1.4462	0.6253	1.0730	1.7776	-10.7294	2.2678

Table 2.5 Parameters of strain hardening model of cold-drawn bars with linear approximation of coefficient c

Grade	a	b	c_4 x 10^8	c_5 x 10^5
Austenitic 1.4401	0.5262	1.0320	6.9332	-2.3727
Lean duplex 1.4162	0.6056	1.0533	8.9375	-3.1295
Duplex 1.4462	0.6360	1.0727	12.4983	-4.9743

Chaboche unified model and parameters for stainless steel bolt

The creep model proposed uses the available stress relaxation test data from Task 5.2. Its implementation in the FE model is however less efficient than the Chaboche model used for the plate material. In order to use the same material model for both plate and bolt material, and increase the efficiency of the whole model, it was decided that SCI would determine the parameters of the Chaboche model using the calibrated strain-hardening creep model from VTT. The identified parameters for austenitic, bolt materials are shown in Table 2.6.

Table 2.6 Chaboche model parameters for austenitic stainless steel bolts

Grade	D [MPa]	n[-]	C_1 [MPa]	γ_1 [-]	C_2 [MPa]	γ_2 [-]	C_3 [MPa]	γ_3 [-]	Q [MPa]	b [-]	k [MPa]
Austenitic 1.4401	200.0	12.0	124738.9	320.2	269288.0	2081.2	595.1	1.0	348.0	1.0	348.0

The calibrated Chaboche model is compared with the strain-hardening creep mode in Figure 2.8. It can be seen that the Chaboche model is also identical to the strain-hardening creep model in terms of tensile stress – strain response and relaxation

behaviour at various stress levels. These comparisons confirm the validity of the Chaboche model for bolt materials.

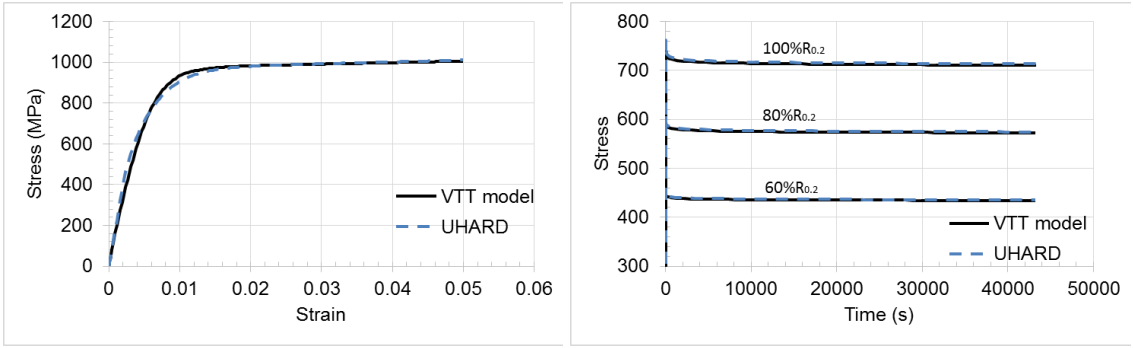

(a) Stress – strain curve (b) Relaxation behaviour

Figure 2.8 Comparison of UHARD and VTT (CREEP) model for austenitic 1.4436 bolt

2.5 Calibration and validation of stainless steel connection models

Slip factor tests were carried out to determine slip factors for different grades of stainless steel with typical surface finishes [2,14]. Four grades of stainless steel were tested: austenitic (A; 1.4404), duplex (D; 1.4462), lean-duplex (LD; 1.4162) and ferritic (F; 1.4003). The visco-plastic material model for the four grades can be found in the previous section. The bolts used in the stainless steel slip resistant connections are M16 BUMAX 88 and 109 bolts produced by BUMAX AB [15]. BUMAX 109 and 88 are comparable to class property of 10.9 and 8.8 according to EN ISO 898-1 [16] for carbon steel bolts.

The slip factor tests were carried out in accordance to EN 1090-2 Annex G. The experimental configuration is identical to the preliminary carbon steel tests presented in the previous chapter (Figure 2.2). Figure 2.9 shows the schematics of the stainless steel preloaded connection to be tested and the FE model which needs to be calibrated. A 40 mm long load cell was used to monitor the change of preload in the bolts throughout the course of the tests. The tests were shared between project partners UDE and TUD. M16 Bumax 88 bolts were used in the tests carried out by UDE while TUD used M16 Bumax 109 bolts. The typical surface finish of the faying surfaces in the tests were: as-rolled (1D), grit blasted (GB) and shot blasted (SB).

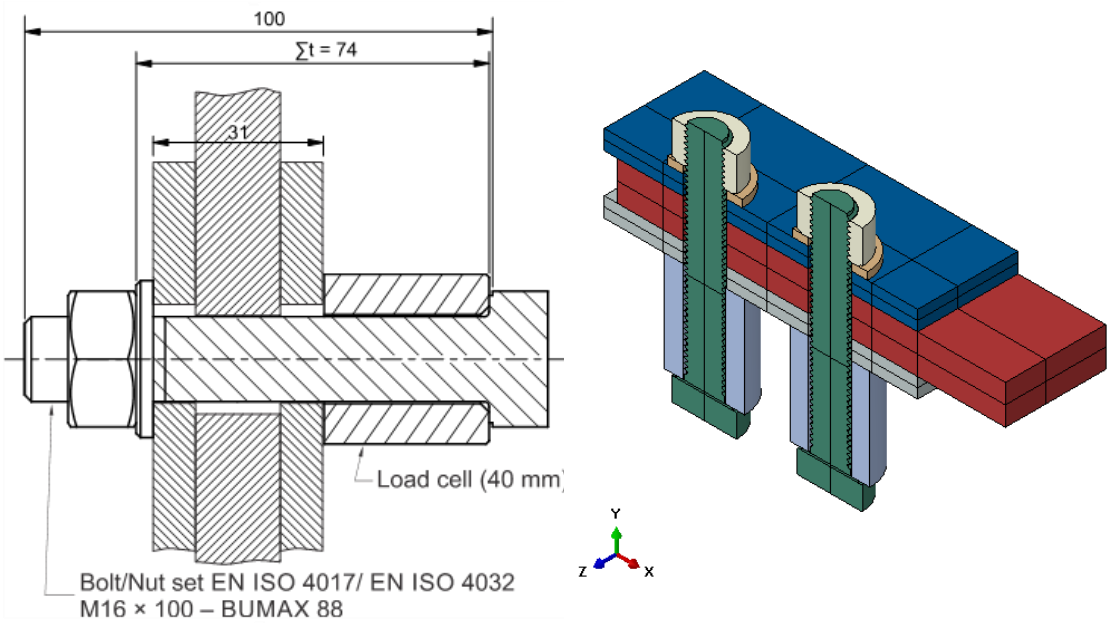

(a) Clamped plates of all bolted connection with load cell (© UDE)

(b) Numerical model of slip-resistant stainless steel connection

Figure 2.9 Numerical model of slip-resistance stainless steel connection

The calibration of the FE model of the stainless steel slip resistant connection was similar to the preliminary study of carbon steel connections. The value of the friction coefficient μ_{fric} was determined so that the nominal slip factor is the same as that measured in the test. Figure 2.10 presents the calibration of the static coefficient of friction for the connection with the grit blasted austenitic plate with M16 Bumax 109 bolts. It was found that by assuming μ_{fric} = 0.6 in the FE model, the slip factor would be the same as the test.

It can be observed in Figure 2.10(a) that the slip response of the FE model is in good agreement with the test results, even though the scatter of the experimental data is relatively large. The loss of preload during the tests is compared in Figure 2.10(b). At the slip of 0.15 mm, the residual preloads in the bolts predicted by the FE model were found to be similar to the test measurements.

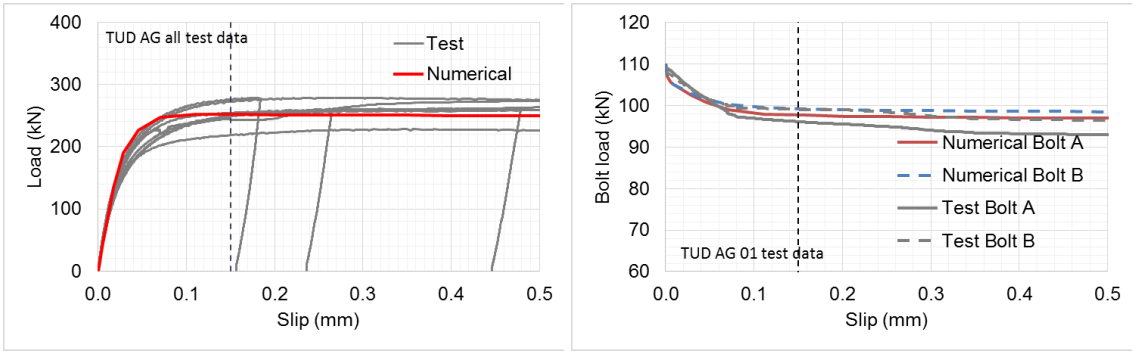

(a) Slip – load curves (b) Loss of preload

Figure 2.10 Calibration results for Austenitic plate with grit blasted surface finish and M16 Bumax 109 bolts (series ID: AG), the static coefficient of friction used for the faying surface was calibrated to be μ_{fric} = 0.60

Calibrations of the FE models against all available test data provided by UDE and TUD are shown in Table 2.7.

Table 2.7 presents the calibrated static coefficient of friction for the four grades of stainless steel with typical surface finishes. The loss of preload at CBG slip of 0.15 mm predicted by the numerical models generally agreed well with the test measurements.

Table 2.7 Summary of tests results and calibration of numerical model

Series ID	Steel grade	Surface finish	$\mu_{ini,mean}$ [4]		$\mu_{act,mean}$ [5]		$\mu_{nom,mean}$ [6]		Loss of preload LP_{mean} [7]		FE μ_s [8]
			Test	FE	Test	FE	Test	FE	Test	FE	
Σt = 74 mm | Σt/d = 4.6 | Bumax 88 M16 bolts | $F_{p,C}$ = 88 kN (UDE)											
A_1D	1.4404	1D[1]	0.21	0.20	0.21	0.21	0.20	0.20	2.1%	4.5%	0.21
A_SB		SB[2]	0.29	0.29	0.30	0.30	0.29	0.29	3.0%	5.0%	0.3
A_GB		GB[3]	0.56	0.56	0.60	0.60	0.56	0.56	7.5%	7.5%	0.6
F_GB	1.4003	GB	0.64	0.64	0.69	0.69	0.65	0.65	6.6%	8.0%	0.71
D_GB	1.4462	GB	0.60	0.59	0.63	0.62	0.60	0.60	4.5%	5.5%	0.62
LD_GB	1.4162	GB	0.51	0.51	0.53	0.53	0.51	0.51	3.7%	5.0%	0.54
Σt = 77 mm | Σt/d = 4.8 | Bumax 109 M16 bolts | $F_{p,C}$ = 110 kN (TUD)											
A_1D	1.4404	1D	0.20	0.19	0.20	0.20	0.19	0.19	1.8%	5.9%	0.2
A_SB		SB	0.33	0.32	0.34	0.34	0.32	0.32	4.1%	6.8%	0.34
A_GB		GB	0.58	0.57	0.65	0.64	0.57	0.57	9.9%	11%	0.64
F_GB	1.4003	GB	0.70	0.68	0.75	0.77	0.68	0.68	8.6%	11.6%	0.77
D_GB	1.4462	GB	0.66	0.66	0.69	0.70	0.66	0.66	5.3%	6.8%	0.705
LD_GB	1.4162	GB	0.63	0.63	0.65	0.68	0.63	0.63	4.6%	6.6%	0.68

[1] as-rolled surface finish | [2] shot blasted surface finish | [3] grit blasted surface finish | [4] mean initial slip factor | [5] mean actual slip factor | [6] mean nominal slip factor | [7] mean loss of preload at 0.15 mm slip | [8] static coefficient of friction between faying surfaces calibrated for the numerical model

The initial, actual and nominal slip factors are evaluated as shown in Equation (5). Since the calibration was based on the nominal slip factors, there were small discrepancies between the initial and actual slip factors produced by the FE model and tests. This discrepancies primarily originated from 1) the initial bolt preload ($F_{p,C,ini}$) achieved at the start of the slip factor tests were always slightly different from the specified value due to uncertainties in the pre-tightening process, and 2) the numerical actual bolt preload ($F_{p,C,act}$) at slip of 0.15 mm also differs from the test measurements. These are also the reasons that the nominal slip factor was used for calibration as the only parameter needs to be varied is the slip load (F_{si}).

$$\mu_{i,ini} = \frac{F_{si}}{4F_{p,C,ini}}, \mu_{i,act} = \frac{F_{si}}{4F_{p,C,act}}, \mu_{i,nom} = \frac{F_{si}}{4F_{p,C,nom}} \quad (5)$$

It can be observed that the static coefficient of friction calibrated for plates with BUMAX 109 bolts are in general greater than for BUMAX 88 bolts. The higher clamping force introduced by the BUMAX 109 bolts is probably a contributing factor, which suggests that, at these contact pressure levels, friction depends on bearing pressure.

It should be noted that the calibration was done using the mean nominal slip factors ($\mu_{nom,mean}$) straight from the tests. The characteristic (final nominal) slip factors recommended in the guidelines [14,17] and the published paper [2], according to EN 1090-2 Annex G, are either taken as the 5% fractile value with a confidence level of 75% or the value determined by a successful extended creep test.

The von Mises stress distributions in the grit blasted austenitic connection at the start and end of the slip factor tests are shown in Figure 2.11.

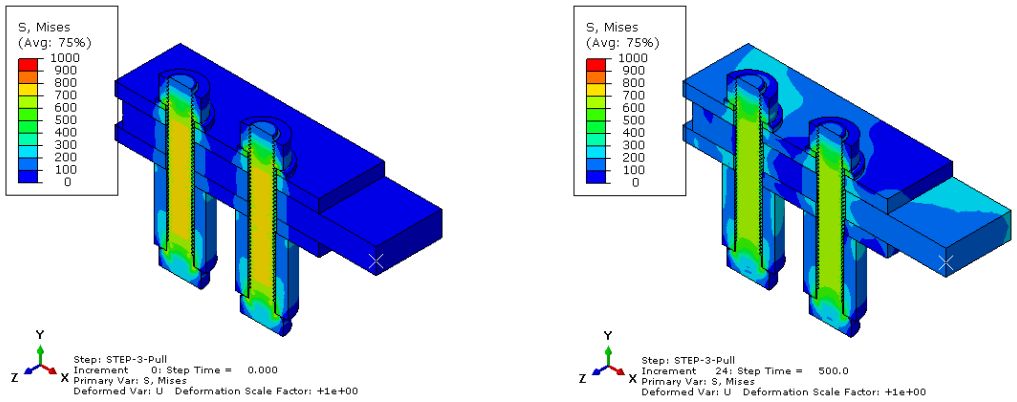

(a) start of slip test (b) end of slip test

Figure 2.11 Stress distribution at the start and end of a slip test (Series ID: AG)

The total plastic strain (including creep strain) distributions in the grit blasted austenitic connection at the start and end of the slip factor tests are shown in Figure 2.12.

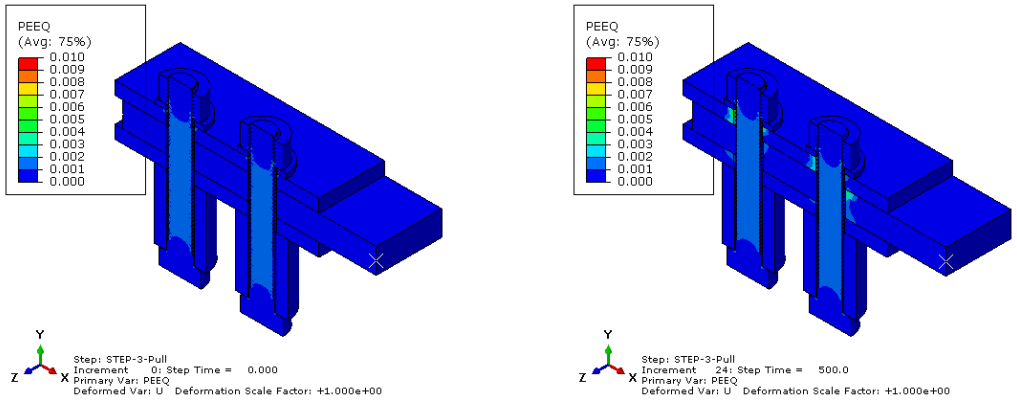

(a) start of slip test (b) end of slip test

Figure 2.12 Inelastic strain distribution at the start and end of a slip test (Series ID: AG)

As an example, the surface compressive contact stress on the surface of the inner and cover plates at the start and end of the slip factor tests are shown in Figure 2.13. It can be seen that the contact stress was in the region of 200-300 MPa throughout the test.

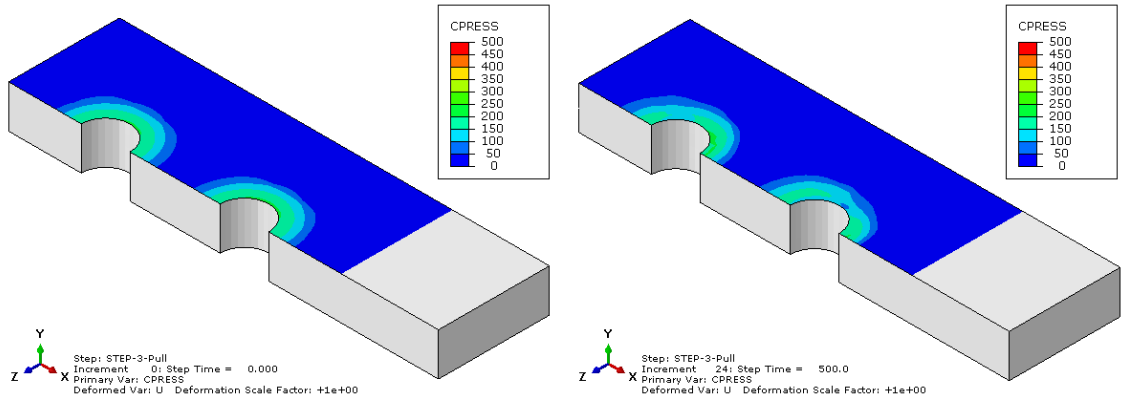

(a) start of slip test (b) end of slip test

Figure 2.13 Surface pressure of inner plate at the start and end of a slip test (Series ID: AG)

2.6 Evaluation of preload loss of bolted assembly model

The FE model of a stainless steel slip resistant connection was validated and the coefficient of friction for various stainless steel grades and typical surface finished were determined. In the validation exercise, the loss of preload during the course of the slip factor tests was also assessed and compared with test measurements. In addition to monitoring bolt preload during the slip factor tests, the relaxation of preloading in stainless steel bolt assemblies was examined in detail in Task 5.3 [18, 19].

Stress relaxation behaviour in stainless steel bars was firstly studied, followed by experimental investigations of the relaxation behaviour of preloaded stainless steel bolted assemblies by UDE. In Task 5.3, austenitic, ferritic, duplex and lean duplex stainless steel bolting assemblies with M16 and M20 bolts were used for measuring the loss of preload of stainless steel bolted connections. The test matrix and test results are summarized in Table 2.8.

All stainless steel plates had the as delivered 1D surface condition without any other surface preparation. Two specimen configurations were developed: (1) one-hole specimen with plate size of 75 mm by 75 mm, and (2) eight-bolt specimen with plate size of 150 mm by 150 mm. Examples of the test specimen are shown in Figure 2.14. The bolts used were A4 austenitic stainless steel M16 and M20 BUMAX 109 and 88. The same bolts were used as those in the slip factor tests introduced previously.

(a) Eight-bolt specimen (150 x 150 mm plate) (b) Single-bolt specimen (75 x 75 mm plate)

Figure 2.14 Test setup of bolt preload relaxation test (© UDE)

In these tests, the same preload level of $F_{p,C} = 0.7f_{ub}A_s$ according to EN 1090-2 ($f_{ub:}$ tensile strength of the bolt, A_s: tensile stress area of the bolt) was considered to compare the influence of different grades of stainless steel and bolt size. As such, the preload levels of M16 BUMAX 109 and 88 were 110 and 88 kN respectively, while M20 BUMAX 88 bolts were pre-tightened to 137 kN.

The preload relaxation test programme provided a good opportunity to examine the validity of the previously proposed visco-plastic stainless steel material model in a more realistic environment, i.e. in a preloaded bolt assembly as opposed to simple material model simulation. The 2D axisymmetric model shown in Figure 2.1 was used in the numerical investigation and compared with the extrapolated results at the end of 50 years. It can be seen from Table 2.8 that the loss of preload predicted by the numerical 2D model compares favourably with test results. It is worth pointing out that more than one test was carried out for each specimen so the maximum and minimum values were tabulated for discussion of the results.

Table 2.8 Predicted loss of preload in bolted assemblies made of stainless steel and comparison with FE results

Specimen ID[1)]	Σt [mm][2)]	Σt/d[3)]	Bolt material	Plate material	Loss of preload after 50 years [%]	
					Test (extrapolated) min/max	FE
SS01	75	3.75	Bumax 88 M20	Austenitic 1.4404	6.0/8.3	7.3
SS02				Ferritic 1.4003	5.4/7.3	7.1
SS03				Duplex 1.4462	5.4/7.2	6.9
SS04				Lean Duplex 1.4162	6.0/9.0	6.8
SS21	59	3.70	Bumax 88 M16	Austenitic 1.4404	6.2/8.5	7.0
SS22				Ferritic 1.4003	5.6/7.7	6.8
SS23				Duplex 1.4462	6.1/8.9	6.7
SS24				Lean Duplex 1.4162	6.2/8.6	6.7
SS26			Bumax 109 M16	Austenitic 1.4404	7.2/9.6	8.8
SS27				Ferritic 1.4003	7.7/9.3	8.7
SS28				Duplex 1.4462	6.4/8.5	8.5
CS	48	2.4	M20 HV-bolt class 10.9	Carbon Steel	7.8/10.5	-

[1)] all bolts were preloaded to the $F_{p,C}$ level | [2)] clamping length | [3)] clamping length to bolt diameter ratio

A graphical representation of the comparison of loss of preload after 50 years is shown in Figure 2.15. It can be seen that the predicted loss of preload from the numerical models satisfactorily fell between the maximum and minimum test values for almost all specimens tested. As a reference, a benchmark test case using M20 HV 109 bolts was included in the study. The comparison with the preloaded carbon steel bolt assembly suggested that the loss of preload in the pre-tensioned stainless steel bolts should not be worse than for a comparable carbon steel bolt.

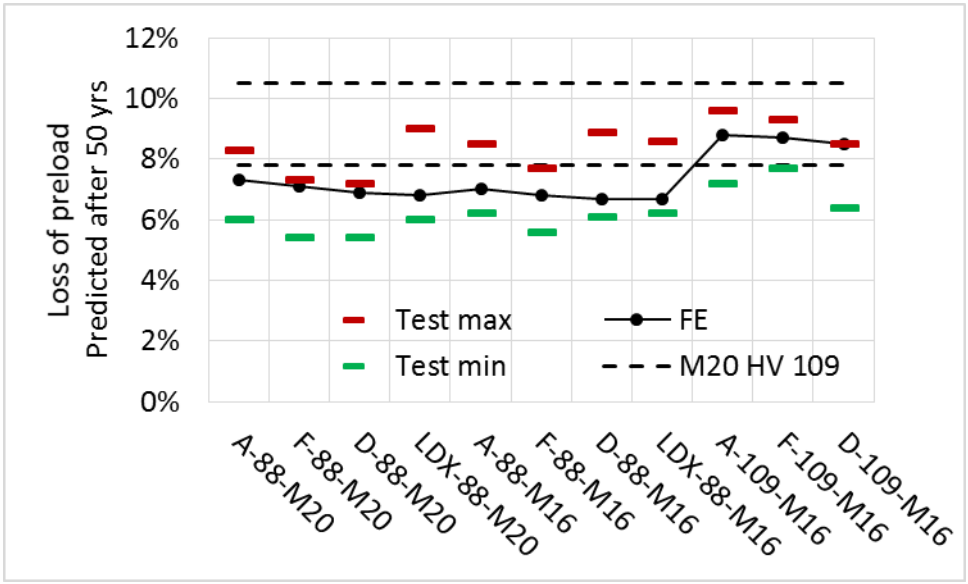

Figure 2.15 Predicted loss of preload after 50 years for stainless steel bolted assembly compared with carbon steel bolts (details refer to Table 2.8)

2.7 Evaluation of long term behaviour of slip resistant stainless steel connection model

In previous sections, the slip resistance connection model has been validated against slip factor tests and the loss of preload in the numerical model was examined using the relaxation tests of bolt assemblies. To complete the evaluation of the numerical models, it is necessary to study the long term response of the slip resistant connection models by comparing them to the extended creep tests carried out in Task 6.2 [2, 14].

Normally extended creep tests are only carried out on a connection which fails the creep tests, i.e. when the connection is subjected to $0.9F_{sm}$ (F_{sm} is the slip load mean value) and the delayed creep exceeds 0.002 mm over a period of 3 hours. In this current project, extended creep tests were additionally conducted on all the series of specimens used in the slip factor tests. The results showed that almost all the creep tests were passed.

The slip factor test model presented in Figure 2.3 was used to model the tests carried out by TUD using M16 BUMAX 109 bolts. Similar to the actual tests, the first step was to pre-tension the bolts to $F_{p,C}$ and in the second step a slip (shear) load of $0.9F_{sm}$ was applied to the inner plate. In the last step the load of $0.9F_{sm}$ was kept constant for 50 years for the numerical model and the final predicted slip displacements were compared against the extrapolated test results.

As can be seen in Figure 2.16 all extended creep tests carried out at TUD were passed. The extrapolated slip displacements at 50 years are all below the 0.3 mm criteria. Slip displacement at the CBG and PE positions after 50 years predicted by the numerical model are also presented here. The numerical CBG slips were found to be typically lower than test measurements.

During the extended creep tests, the preload in the bolts was continuously measured. Figure 2.17 shows the course of the preload during the tests on the BUMAX 109 bolts. The graphs show the application of the preload, the losses during the 30 minutes waiting

period, the losses during the application of the extended creep load (F_{ect}) and the losses during the period of the extended creep test (ranges from 7 – 79 days). A linear extrapolation was used to predict the slip after 50 years.

The preload time history over 50 years predicted by the numerical models is also plotted and compared with test measurements in Figure 2.17. It can be seen that at each stage the preload in the numerical models agreed reasonably well with the test records.

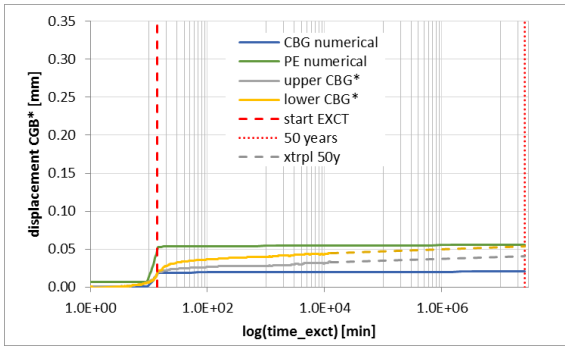

(a) Austenitic plates with 1D surface (A1D)

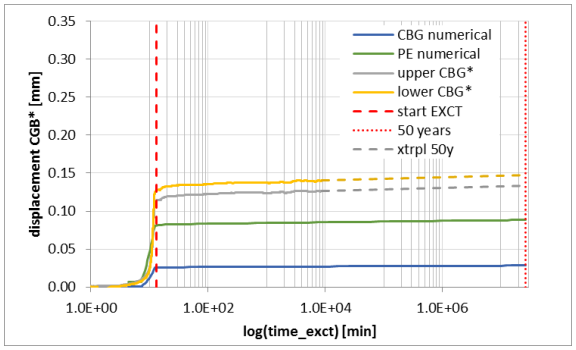

(b) Austenitic plates with shot blasted surface (AS)

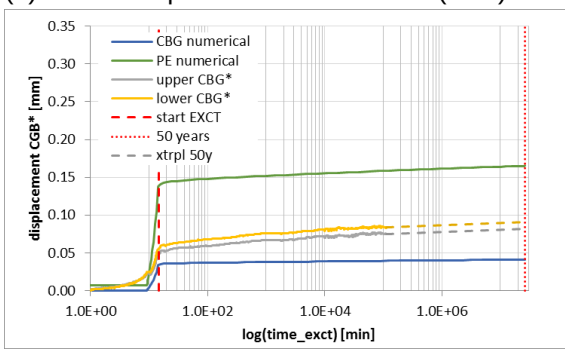

(c) Austenitic plates with grit blasted surface (AG)

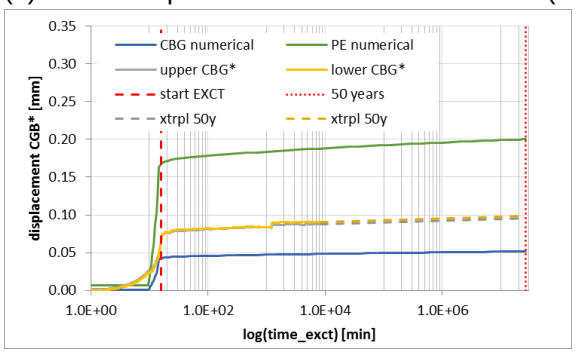

(d) Ferritic plates with grit blasted surface (FG)

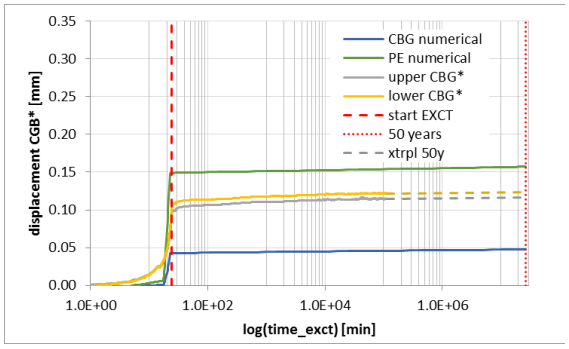

(e) Duplex plates with grit blasted surface (DG)

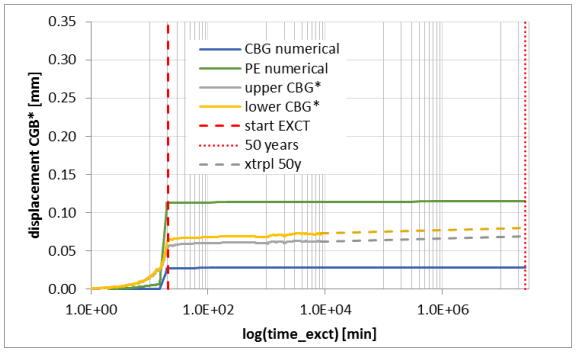

(f) Lean duplex plates with grit blasted surface (LG)

CBG* - During the ECT tests, slip was only measured at the PE position, so slip at CBG was calculated based on the relation between PE and CBG measurements found in the static slip tests

Figure 2.16 Comparison of numerical model with extended creep tests results considering different stainless steel grades and surface conditions, test series with bolts of property class 10.9 (Bumax 109)

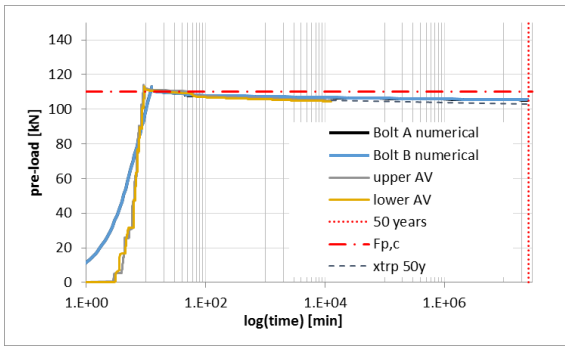

(a) Austenitic plates with 1D surface (A1D)

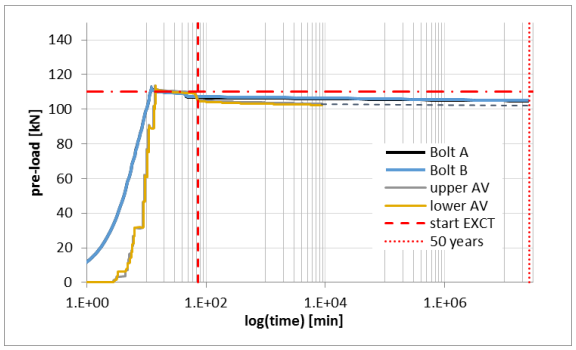

(b) Austenitic plates with shot blasted surface (AS)

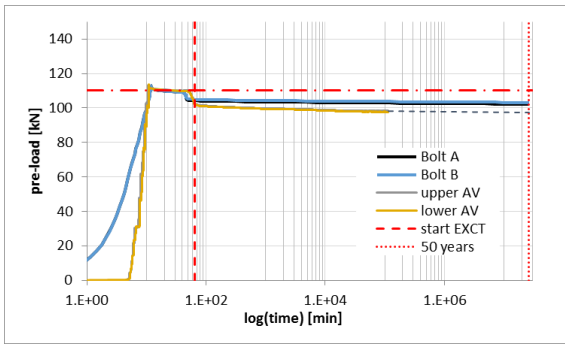

(c) Austenitic plates with grit blasted surface (AG)

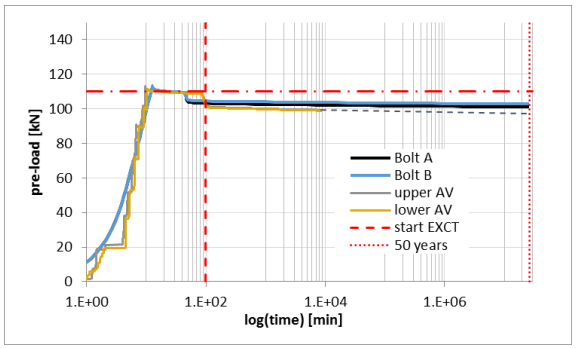

(d) Ferritic plates with grit blasted surface (FG)

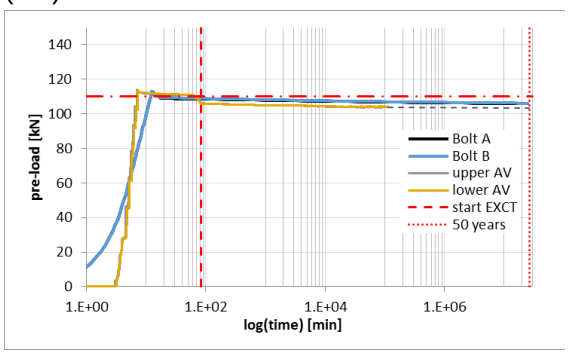

(e) Duplex plates with grit blasted surface (DG)

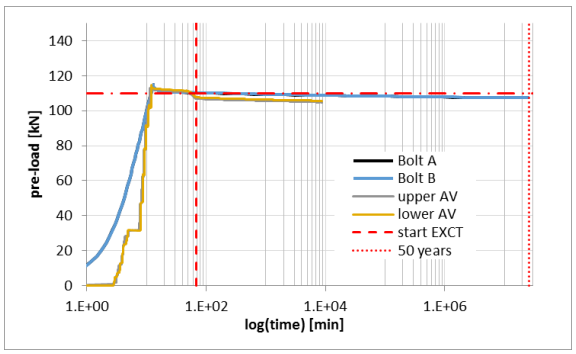

(f) Lean duplex plates with grit blasted surface (LG)

Figure 2.17 Comparison of numerical model with time history of the bolt preload during extended creep tests – with bolts of property class 10.9 (Bumax 109)

A summary of the comparison of the extended creep test results is presented in Table 2.9. It can be observed that after 50 years the loss of preload in the numerical models compares reasonably well to the test results.

However, the slip displacement at the CBG position after 50 years predicted by the FE models are smaller than the test data. This may suggest that most of the slip occurred at the frictional surface due to high contact stress induced by visco-plastic deformation. The stainless steel plate and bolt material do not suffer from any significant creep/stress relaxation and therefore do not contribute to the development of slip over the long term. The FE model of the extended creep test assumed a constant frictional coefficient and was only able to predict the long term creep/stress relaxation occurring in the plate and bolt material.

Table 2.9 Evaluation of numerical model for long term loss of bolt preload and slip behaviour in extended creep tests

Spec. ID	F_{ect}[1)] (kN)	Plate		Loss of preload (%) [test/FE]	CBG slip (mm) [test/FE]		
		Grade	Surface finish		start	at 50 yrs	increase over 50 yrs
A_1D	70	1.4404	as-rolled	8-9 / 5.9	0.018 / 0.019	0.047 / 0.02	0.029 / 0.001
A_SB	122		shot blasted	9-10 / 6.4	0.116 / 0.025	0.141 / 0.028	0.025 / 0.003
A_GB	210		grit blasted	9 / 8.4	0.053 / 0.034	0.086 / 0.041	0.033 / 0.007
F_GB	260	1.4003		8 / 9.4	0.068 / 0.042	0.097 / 0.052	0.029 / 0.010
D_GB	260	1.4462		7-8 / 6.2	0.089 / 0.043	0.120 / 0.047	0.031 / 0.004
LD_GB	215	1.4162		7-8 / 6	0.058 / 0.027	0.074 / 0.029	0.016 / 0.002

[1)] extended creep test load and F_{ect} =0.9 F_{sm}

2.8 Conclusion of numerical model validation

In Chapter 2, the FE models and the visco-plastic material models used in current project are briefly introduced. Details of the models and their development can be found in Deliverable 5.6 [9,20]. The main efforts were placed on validation of the stainless steel connection slip factor test models and their long term behaviour.

A series of carbon steel connection tests were used at the early stage of the work to check the response of the model was consistent with the physical test specimen. Later on, the slip factor test model complete with visco-plastic material model were extensively studied and validated against slip factor tests results of stainless steel connections.

Values for the static coefficient of friction for various grades of stainless steel with typical surface finishes were calibrated against test data. Subsequently, the long term behaviour of the numerical models was validated and evaluated by comparing with experimental results as well. The models developed in this project are shown to be able to accurately predict the slip factors of stainless steel slip resistant connections and their long term time dependent behaviour.

3 SLIP FACTOR CORRECTION

The usage of a load cell to monitor loss of preloading in bolts resulted in longer clamping lengths of the test specimen than specified in EN 1090-2 Annex G. As discussed before, the loss of preload and subsequently the resistance and slip factors are affected by the longer clamping length. A theoretical method [21] was proposed in D1.2 of SIROCO project to compensate for the influence of the clamping length of the bolts on the results of slip factor tests. Using this method, the nominal slip factor which would have been obtained according to EN 1090-2 Annex G (i.e. without the load cell, hence shorter or standard clamping length and more relevant to actual connections) can be obtained.

The correction factor C_{cl} to derive the slip factors for a short bolt/clamping length from long bolts/clamping length is defined as below:

$$C_{cl} = \frac{1-R}{1-r} \qquad r\ is\ the\ loss\ of\ preload$$

$$R = r \times R_a \times \frac{\delta_{s,0}}{\delta_{s,1}}, \qquad R_a = \frac{\alpha_1}{\alpha_1 + 1} \cdot \frac{\alpha_0 + 1}{\alpha_0}, \qquad \alpha_0 = \frac{\delta_{s,0}}{\delta_{p,0}}, \alpha_1 = \frac{\delta_{s,1}}{\delta_{p,1}} \tag{6}$$

In above equations, subscripts 0 denotes properties or characteristics of the long bolts while 1 denotes the short bolts whose results are derived from the long bolts through the correction factor C_{cl}. δ_s is the resilience of bolts and δ_p is the resilience of the clamped plate in a bolted assembly as defined in Appendix A. It should be noted that the resilience of the bolts and clamped plates is used instead of stiffness to obtain the correction factors.

Limited validation of the theoretical method was undertaken in [21] using the slip factor tests on carbon steel connections with different clamping lengths (discussed in Section 2.2). The objective of this study is to use the validated FE models to evaluate the accuracy of the proposed theoretical method and to adjust the slip factors obtained with a load cell.

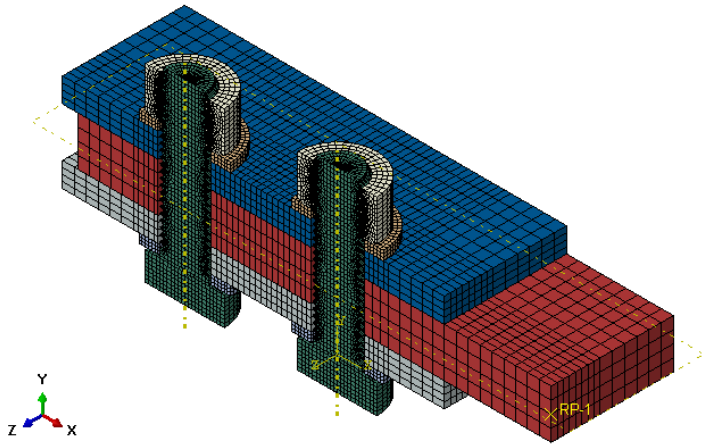

Figure 3.1 Meshed numerical model of slip factor test configuration specified by EN 1090-2 Annex G (M16 bolt)

Figure 3.1 presents the FE model according to EN 1090-2 Annex G. In the absence of the load cell, the total clamping length, including the washers, for an M16 bolt connection is 38 mm. The clamping length of the test specimen prepared by TUD, including the load cell and washers, was approximately 77 mm. The corrected nominal slip factors obtained by the FE model and theoretical method are compared in Table 3.1.

Table 3.1 Comparison of slip factor correction (M16 BUMAX 109 bolts, TUD)

Test ID	$r^{1)}$ [%]	$C_{cl}^{2)}$	$\mu_{nom,0}^{3)}$	$\mu_{nom,1,corr}^{4)}$	$\mu_{nom,1,FE}^{5)}$	$Error^{6)}$ [%]
A_1D	8.1	0.95	0.19	0.18	0.19	-5.0
A_SB	8.1	0.95	0.32	0.30	0.31	-1.9
A_GB	8.6	0.94	0.57	0.54	0.54	0.0
F_GB	8.6	0.94	0.68	0.64	0.63	1.5
D_GB	8.6	0.94	0.66	0.62	0.65	-4.6
LD_GB	8.6	0.94	0.63	0.59	0.63	-6.0

[1)] preload loss during slip test with long bolts (clamping length of 77 mm)

[2)] correction factor

[3)] calibrated slip factor with long bolts (e.g. with load cell)

[4)] corrected slip factor (for standard/short bolt length, clamping length of 38 mm)

[5)] numerical slip factor with standard/short bolt (clamping length of 38 mm)

[6)] difference between numerical value and corrected value ([4)-5)/5)])

From Equation (6) it can be seen that the correction is based on primarily the plate and bolt resilience (δ) of long and short (standard) clamping length and the loss of bolt preload (r) under slip load. Resilience of the plates and bolts and the loss of preload can be estimated according to VDI 2230-1, as illustrated in Appendix A.

The corrected slip factor then can be estimated as $\mu_{nom,1,corr} = C_{cl} \times \mu_{nom,0}$. The nominal slip factors ($\mu_{nom,1,FE}$) estimated using the FE model (standard clamping length) shown in Figure 3.1 are also presented. The comparison shows that the corrected slip factors are in good agreement with the numerical values. It suggests that the proposed theoretical method can be used to accurately adjust the slip factors obtained with longer bolt length than the standard specified by EN 1090-2 Annex G.

4 PARAMETRIC STUDY

In previous chapters, numerical models of stainless steel slip resistant connections have been validated against test results and studied extensively for their long term visco-plastic behaviour.

The models developed and validated previously were used in the parametric study to check the suitability of the slip factors obtained from the test programme and make recommendations for the application of the slip factors. A large number of cases with different geometric and material parameters were studied. Parametric studies included simulation of both slip factor tests and extended creep tests. The effect of different parameters on the slip factor, final slip and loss of preload after 50 years were examined.

Geometric properties of slip test specimens only using M16 and M20 bolts are specified in EN1090-2 Annex G, with a plate thickness to bolt size ratio of 2. In the current parametric studies, dimensions of the connection assembly were adjusted proportionally according to key geometric parameters (e.g. bolt size or plate thickness). As a results, the relative size of the components are similar to the EN 1090-2 specification.

Five key parameters were studied: 1) bolt size, 2) plate thickness to plate thickness ratio (Σt/d), 3) plate material and surface finishes, 4) bolt material and 5) bolt property class.

Bolt size

Stainless steel bolts of size M16 were used in the test programme. In this parametric study, the bolt sizes to be considered are: M12, M16, M20, M24, M30 and M36. The bolts were all modelled according to EN ISO 4017 [22].

Plate thickness to bolt size ratio (Σt/d)

Due to the inclusion of load cell in the tests, the clamping length to bolt size ratio was increased to 4.8 from 2.4 as specified by EN 1090-2 Annex G for an M16 bolt. For simplicity in this parametric study, the plate thickness to bolt size ratio to be studied are: 1, 2, 4, 6 and 8. The thickness of the washers are excluded here. The nominal thickness or the clamping length (including all plates and washers) will be slightly larger.

Plate material and surface finish

Four types of stainless steel plate material with typical surface finishes have been tested in the project. Based on the tests, the material and surface finish considered in the parametric study are: A1D (austenitic with as-rolled surface), AS (austenitic with shot blasted surface), AG (austenitic with grit blasted surface), FG (ferritic with grit blasted surface) and DG (duplex with grit blasted surface).

Lean duplex was not included in the parametric study as it is expected to be similar to duplex stainless steel.

All bolts in the parametric study were preloaded to Fp,C and the static coefficient of friction was selected according to the plate material, surface finish and bolt property class (based on Table 2.7). Austenitic bolts were used throughout the study. The preloading speed was assumed to be 10 RPM for all models.

The total number of cases to be simulated in the parametric matrix exceeds 1000 and would take a few months to complete. In order to reduce the size of the matrix and complete the simulation work within a realistic time frame, the matrix has been broken

down to small matrices. Each matrix focused on one combination and limited parameters were considered.

In addition to the above parameters, the surface friction coefficient and bolt preload level were also investigated.

4.1 Plate thickness to bolt size ratio

The first matrix focused on the effect of plate thickness to bolt size ratio on the response of the slip resistant connection. Three bolt sizes selected were: M12, M20 and M36. Austenitic plate with grit blasted surface and BUMAX 88 bolts were used in the study.

The matrix can be summarized as (M12, M20, M36) × (1, 2, 4, 6, 8) × (AG) × (A) × (8.8) = 15. The total number of cases to be studied are 30, including the slip factor tests and extended creep tests.

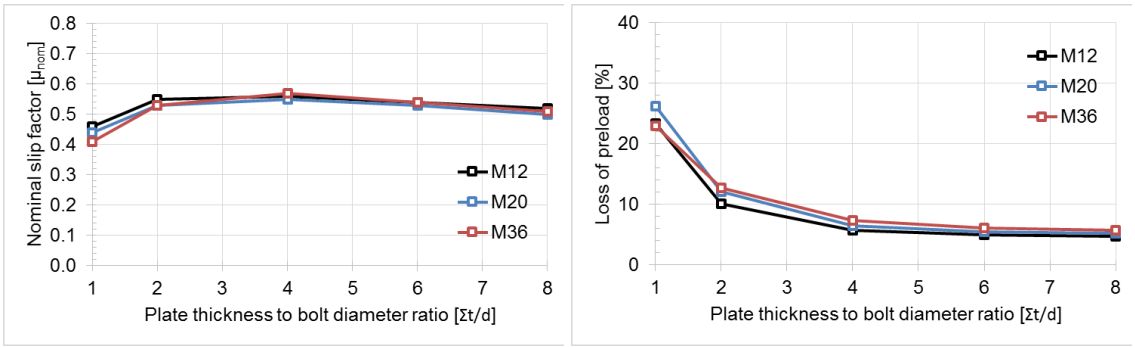

(a) Nominal slip factors (b) Loss of preload at 0.15 mm slip

Figure 4.1 Effect of plate thickness to bolt size ratio on the behaviour of stainless steel slip resistant connections (A88, M20, AG plate),

The effect of plate thickness to bolt size ratio on the slip factor achieved and loss of preload can be observed in Figure 4.1. For the same plate surface finishes the achieved slip factor decreases when the thickness to bolt size ratio is less than 2. This is mainly due to the large loss of preload at low thickness to bolt size ratio shown in Figure 4.1(b).

Higher slip factors can be achieved when the ratio is 2 – 4 but beyond this range the slip factor starts to reduce slightly again. The reduction in the nominal slip factor (or the slip resistance) can be explained by the comparison of contact stress shown in Figure 4.2. At thickness to bolt size ratio of 2, it can be seen from Figure 4.2(a) that part of the relatively thin plates separated under the bolt preload and this resulted in a small region of high contact pressure around the bolt holes. The area of high contact pressure started to enlarge as the plate thickness increased (i.e. less separation between plates), as shown in Figure 4.2(c) – (d). However, the intensity of the compressive stress reduced due to larger contact area. The larger contact area with low contact stress contributed to the small reduction of the slip resistance at high thickness to bolt size ratio ($\sum t/d \geq 4$).

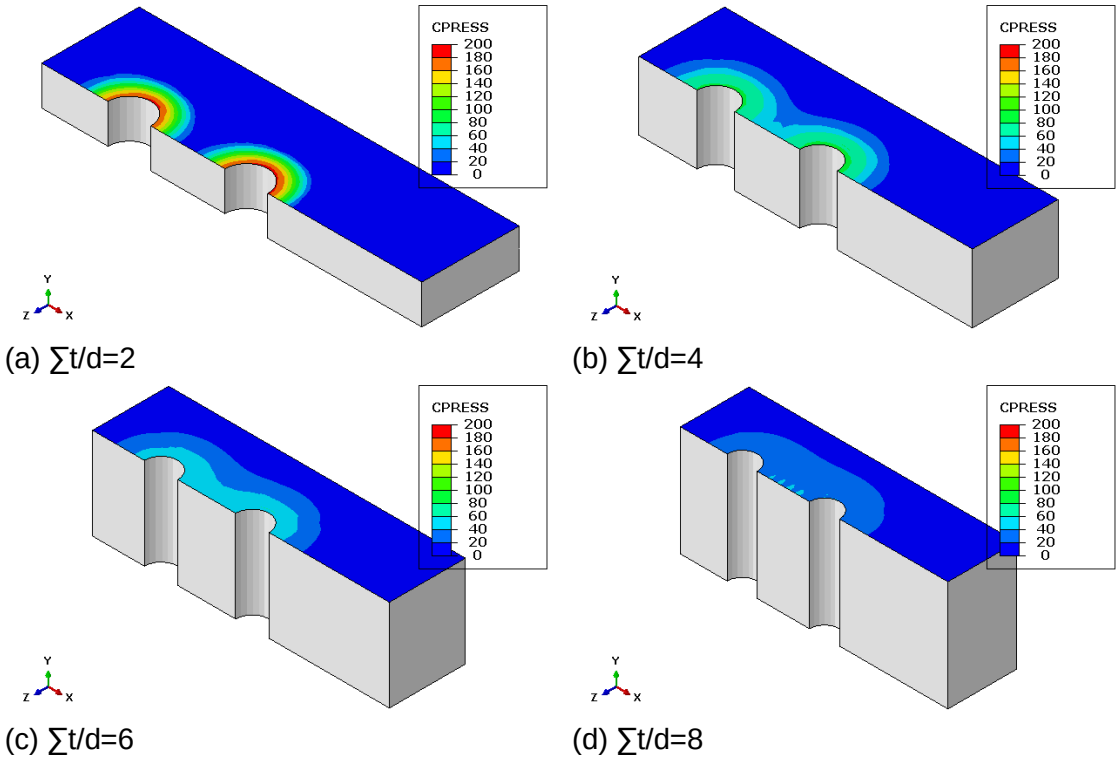

(a) ∑t/d=2 (b) ∑t/d=4

(c) ∑t/d=6 (d) ∑t/d=8

Figure 4.2 Comparison of contact stress on the faying surface of the inner plate after preload (A88, M20, AG plate), unit: MPa

The loss of preload was reduced when the thickness to bolt size ratio increased. From observing these results, it is possible that the loss of preload would approach a limiting value at a large thickness to bolt size ratio.

Figure 4.3 presents the effect of the plate thickness to bolt size ratio on the long term behaviour of the bolt. The results were taken from the extended creep simulation of the parametric study. It can be seen that the slip at the CBG position after 50 years was less than the 0.3 mm criteria for all thickness to bolt size ratios. The loss of preload in the bolts was also predicted to be around 10 % (except in the case of ∑t/d=1) after 50 years. Both loss of preload and CBG slip after 50 years would decrease when the thickness to bolt size ratio increased.

It should be noted that the extended creep tests were used in the parametric study to show the effect of the plate thickness to bolt size on the slip after 50 years. It was not intended to determine the slip as the numerical model would also produce a smaller slip over the long term due its inability to model the creep/visco-plastic deformation at a micro level on the faying surface (as discussed in Section 2.7).

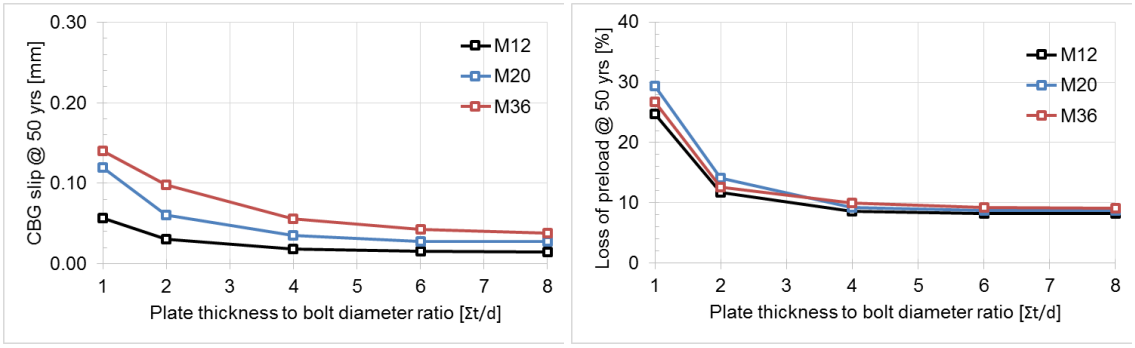

(a) CBG slip after 50 years (b) Loss of preload after 50 years

Figure 4.3 Effect of plate thickness to bolt size ratio on the long term response of a stainless steel slip resistant connection(A88, M20, AG plate),

4.2 Bolt size

The second matrix focused on the effect of bolt size on the slip factor and the long term response of the connection. Plate thickness to bolt size ratio of 2 and 6 were chosen in the study. For consistency, austenitic plate with grit blasted surface and BUMAX 88 bolts were used in the study as well.

The matrix can be summarized as (M12, M16, M20, M24, M30, M36) × (2,6) × (AG) × (A) × (8.8) = 12. The total number of cases to be studied is 24, including slip factor tests and extended creep tests.

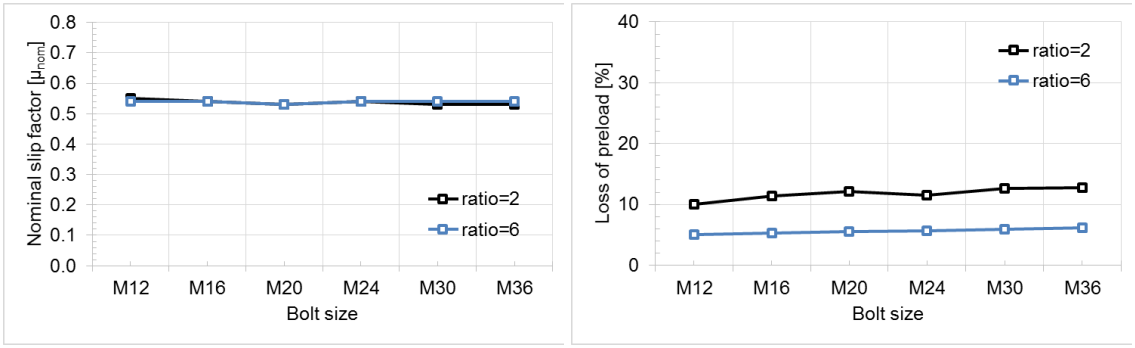

(a) Nominal slip factors (b) Loss of preload at 0.15 mm slip

Figure 4.4 Effect of bolt size on the long term behaviour of a stainless steel slip resistant connection (A88, AG plate, ∑t/d=2)

The effect of plate thickness to bolt size ratio on the slip factor achieved and loss of preload can be observed in Figure 4.1. Plate thickness to bolt size ratio of 2 and 6 were selected in the analysis. It is shown that the size of bolts did not have any meaningful influence over the nominal factor achieved by the stainless steel slip resistant connection models. Slightly higher loss of preload can be observed at larger bolt sizes.

The comparison shown in Figure 4.5 illustrates that the contact stresses (hence the friction) between the faying surfaces are almost identical for connections using M16 and M36 bolts. While larger bolts introduce higher preload, the contact area is also larger. The resulting contact stress remains almost constant and this is the reason that the slip factors do not change with different sizes of bolts provided that other factors remain the same.

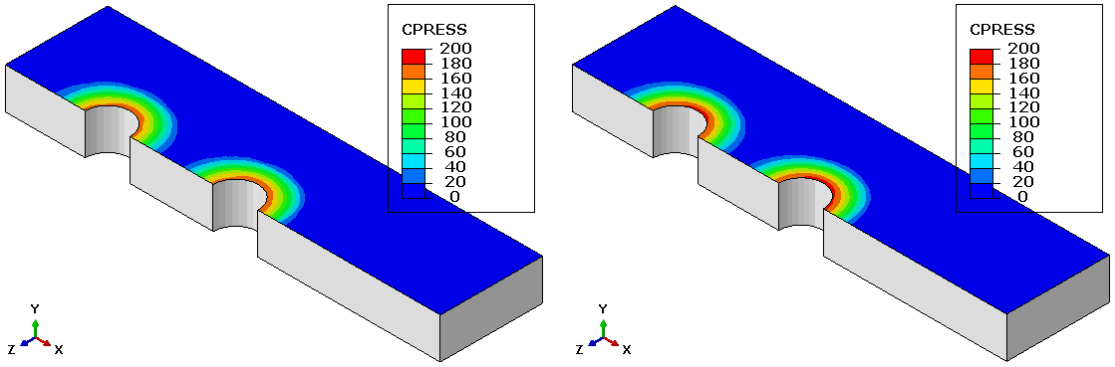

(a) M16 bolts (b) M36 bolts

Figure 4.5 Comparison of contact stress on the faying surfaces of the inner plate after preload (A88, AG plate, ∑t/d=2), unit: MPa

The long term behaviour of the connection models with different size of bolts are shown in Figure 4.6. It can be seen that larger bolts resulted in higher CBG slip at 50 years but none of the results exceeded the 0.3 mm criteria. Loss of preload wereas around 10% after 50 years.

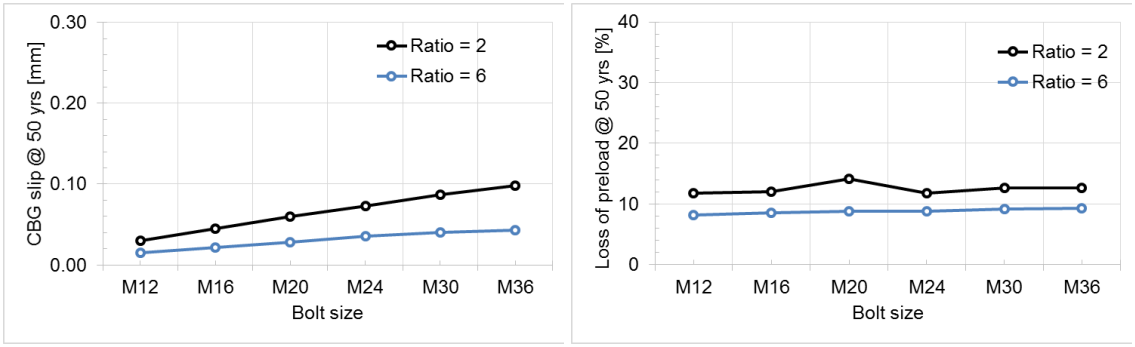

(a) CBG slip after 50 years (b) Loss of preload after 50 years

Figure 4.6 Effect of bolt size on the long term behaviour of a stainless steel slip resistant connection (A88, AG plate)

4.3 Surface (static coefficient of friction)

Section 2.5 presents the calibration of static coefficient of friction for four types of stainless steel plates with typical surface finish. The effect of the static coefficient of friction of the faying surface on the behaviour of the slip resistant connection is studied here.

The parametric study can be summarized as ($\mu_1 = 0.1$, $\mu_2 = 0.2$, $\mu_3 = 0.3$, $\mu_4 = 0.4$, $\mu_5 = 0.5$, $\mu_6 = 0.6$, $\mu_7 = 0.7$, $\mu_8 = 0.8$) × (M20) × (2) × (A) × (A) × (8.8) = 8. Eight friction coefficients were included in the study. Both the plates and bolts were assumed to be austenitic. The size and property class of the bolt are M20 and 8.8. The surface finish of the plate was not specified since the friction coefficient was the variable in the parametric study.

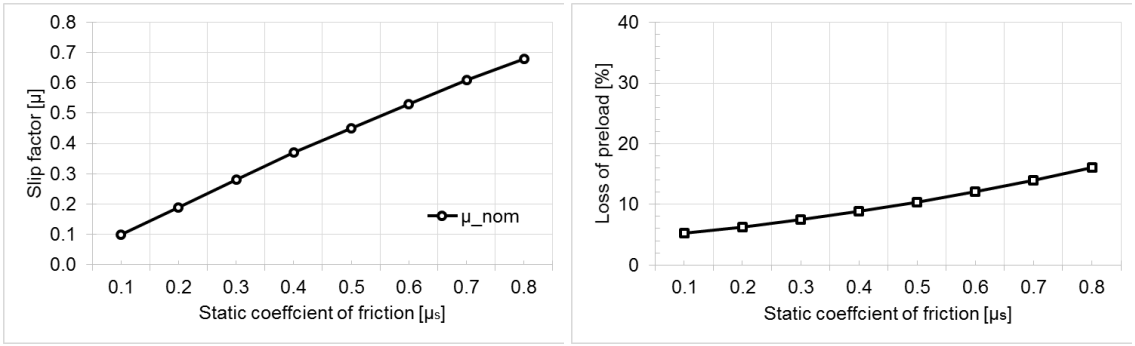

(a) Slip factors (b) Loss of preload at 0.15 mm slip

Figure 4.7 Effect of friction coefficient on the behaviour of a stainless steel slip resistant connection (bolt: A88 M20, plate: A, ∑t/d=2)

The effect of friction coefficient on the response of preloaded bolted connections are presented in Figure 4.7. As expected, higher friction coefficient undoubtedly results in higher nominal slip factors and higher loss of preload at slip of 0.15 mm.

The long term behaviour with different friction coefficients is shown in Figure 4.8. Higher friction resulted in greater CBG slip and higher loss of preload after 50 years. This is due to the high stress introduced in the components by higher friction between the faying surfaces, and higher stress will result in more creep/stress relaxation in visco-plastic materials.

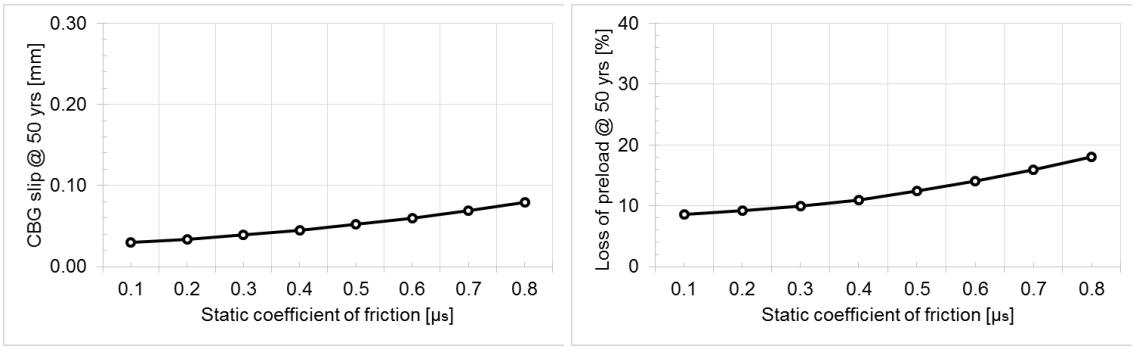

(a) CBG slip after 50 years (b) Loss of preload after 50 years

Figure 4.8 Effect of friction coefficient on the long term behaviour of a stainless steel slip resistant connection bolt: A88 M20, plate: A, ∑t/d=2)

4.4 Bolt preload level

Extensive investigations were carried out on the tightening and preloading behaviour of EN ISO 4014 and EN ISO 4017 bolting assemblies. The tests showed that specified preloading levels, such as $F_{p,C}$ and $F_{p,C}^*$ can be achieved with sufficient reliability using a suitable lubricant. This parametric study studied the effect of the bolt preload on the short and longer term behaviour of stainless steel slip resistant connections.

Four bolt preload levels were studied and the matrix can be summarized as: ($1.1F_{p,C}$ = 151 kN, $F_{p,C}$ = 137 kN, $F_{p,C}^*$ = 109 kN, $0.9F_{p,C}^*$ = 98 kN) × (M20) × (2) × (AG) × (A) × (8.8) = 4.

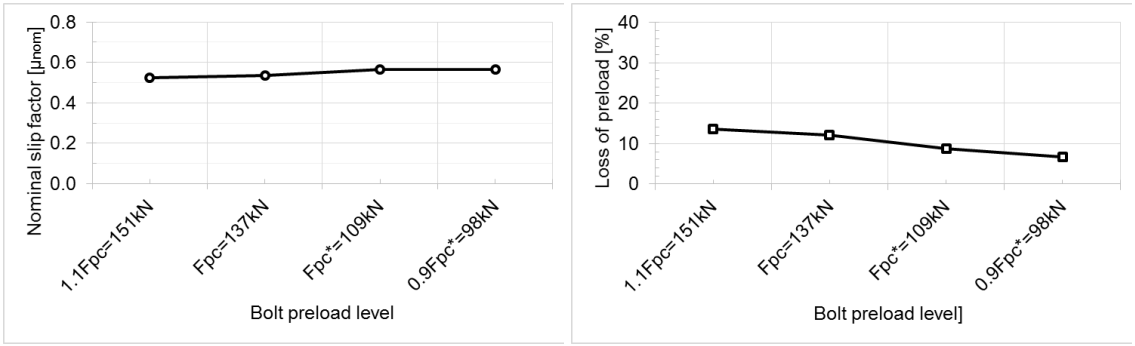

(a) Nominal slip factors (b) Loss of preload at 0.15 mm slip

Figure 4.9 Effect of bolt preload on the behaviour of a stainless steel slip resistant connection (bolt: A88 M20, plate: AG, ∑t/d=2,)

The effect of bolt preload on the slip factor and loss of preload are shown in Figure 4.9. It can be seen that the nominal slip factors were not affected significantly by the reduction of the bolt preload level, but the loss of preload reduced slightly when lower preload was used. It can be seen that there is a small increase in the nominal slip factor as the preload was reduced. This is mainly because the friction coefficient in the current modelling study was fixed but in reality it is dependent on the contact pressure. The lower friction coefficient as a result of smaller preload would keep the slip factor roughly constant between the four preload levels.

As shown in Figure 4.10, both the long term slip and loss of preload after 50 years was reduced with lower bolt preload. This is mainly due to the lower stress in the components as a result of low preload.

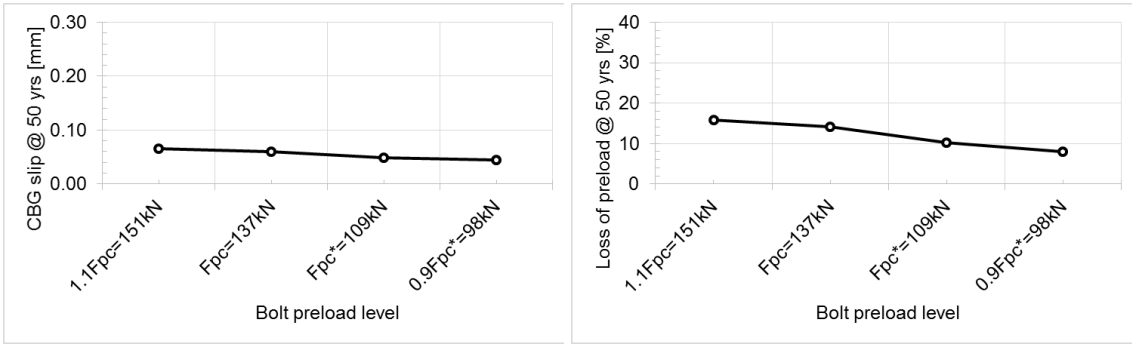

(a) CBG slip after 50 years (b) Loss of preload after 50 years

Figure 4.10 Effect of bolt preload on the long term behaviour of a stainless steel resistant connection (bolt: A88 M20, plate: AG, ∑t/d=2)

5 CONCLUSIONS AND RECOMMENDATIONS

The numerical model developed in work package 5 [20] was extended with a surface friction model and calibrated against slip factor tests of stainless steel preloaded bolted connections in this current work package. The slip response and long term behaviour of the numerical models has been also evaluated by comparison against relaxation and extended creep tests of bolted assemblies. It was shown that the numerical model is able to accurately predict both short and long term behaviour of stainless steel slip resistant connections.

The validated numerical models have been subsequently used in parametric studies to extrapolate the test results. The parametric studies focused on different geometric and material parameters, surface friction coefficient and bolt preload levels. The numerical results were presented and discussed in this report.

Based on the numerical study, some observations and recommendations can be made for the design and use of stainless steel slip resistant connections:

- Preload loss was around 10% or less as found out in the parametric study. Due to the relatively high loading speed of 10 RPM the loss of preload would be higher than in practice.
- Plate thickness to bolt diameter ratio should be between 2 – 4 to achieve the desired slip factors, although a longer clamping length would reduce the loss of preload.
- Bolt size does not affect the slip resistance of the connection, but in order to minimise long term creep, smaller bolts should be used.
- Reducing the preload level does not lead to lower nominal slip factors. However, as the friction is dependent on the bearing pressure between the faying plates, it is recommended to use the slip factor which has been determined by the same level of preload in the slip factor test. As a result, the recommended slip factors from this project should only be used for preload level of $F_{p,C.}$

The calibrated model has also been successfully used to compensate for the effect of the long clamping length of the test specimen due to inclusion of the load cell. The corrected slip factors produced by FE models are in good agreement with the theoretical method.

The numerical model presented in the current study assumed a constant friction coefficient between the faying surfaces. It would be beneficial in future work to use a more complicated friction model which can be made dependent on contact pressure and time. This should improve the accuracy of the numerical model for predicting both the short and long term behaviour of stainless steel slip resistant connections.

6 REFERENCES

[1] SIROCO D6.2: Slip factors for typical stainless steel surface finishes and new types of coatings for stainless steel, 2017

[2] Stranghöner, N., Afzali, N., de Vries, P., Schedin, E., Pilhagen, J., Cardwell, S., Slip-resistance bolted connections of stainless steel, Steel Construction 10 (2017), No.4, pp333-343

[3] Execution of steel structures and aluminium structures, Part 2: Technical requirements for steel structures, BS EN 1090-2: 2008

[4] SIROCO D5.4: Preloading behaviour and preloading levels for stainless steel bolt assemblies including relaxation with detailed specifications for recommended preloading methods, 2017

[5] Stranghöner, N., Jungbluth, D., Abraham, C., Söderman, Ą., Tightening behaviour of preloaded stainless steel bolding assemblies, Steel Construction 10 (2017), No.4, pp319-332

[6] Hexagon head bolts. Product grades A and B. BS EN ISO 4014:2011

[7] Hexagon head screws. Product grades A and B. BS EN ISO 4017:2001

[8] SIROCO D5.6 Report on numerical model calibration: Hradil, P., Sippola, M., Manninen, T., Baddoo N. and Chen, A., WP5: Preloading Of stainless steel bolts, 2017

[9] Hradil, P., Sippola, M., Manninen, T., Baddoo N. and Chen, A., Numerical modelling of stainless steel preloaded bolted connections, Steel Construction 10 (2017), No.4, pp344-353

[10] SIROCO D5.2: Report on creep and stress relaxation behaviour of stainless steel plates, OSOY

[11] SIROCO D5.3: Report on creep and stress relaxation behaviour of stainless steel bars and bolts, OSAB

[12] Annex G Test to determine slip factor, Part 2: Technical requirements for steel structures, Execution of steel structures and aluminium structures BS EN 1090, 2008

[13] Systematic calculation of high duty bolted joints VDI 2230 Part 1, Verein Deutscher Ingenieure, Dusseldorf, 2003

[14] SIROCO D6.2: Slip factors for typical stainless steel surface finishes and new types of coating for stainless steel, TUD

[15] http://www.bumax-fasteners.com/technical-information/bumax-grades/

[16] EN ISO 898-1:2013, Mechanical properties of fasteners made of carbon steel and alloy steel – Part 1: Bolts, screws and studs with specified property class – Coarse thread and fine pitch thread

[17] SIROCO D6.4: Design recommendations and design examples, SCI

[18] SIROCO D5.4 Preloading behaviour and preloading levels for stainless steel bolt assemblies including relaxation with detailed specification for recommended preloading methods, UDE

[19] Afzali, N., Pilhagen, J., Manninen, T., Schedin, E., Stranghöner, N., Preload losses in stainless steel bolting assemblies, Steel Construction 10 (2017), No.4, pp310-318

[20] SIROCO D5.6: Report on numerical model calibration, VTT-R-01467-17, VTT, Finland, 2017

[21] SIROCO D1.2: Vries, P.A. de, Nijgh, M.P., Influence of the test speed in slip factor tests. Delft University of Technology, report 6-18-01, Stevin Laboratory, 2018

[22] EN ISO 4017:2014, Fasteners – Hexagon head screws – Product grades A and B (ISO 4017:2014)

APPENDIX A LOSS OF PRELOAD (VDI 2230-1)

The procedure for calculating the bolt and clamped part resilience and loss of preload in a single bolt according to VDI 2230-1 [13] is shown below.

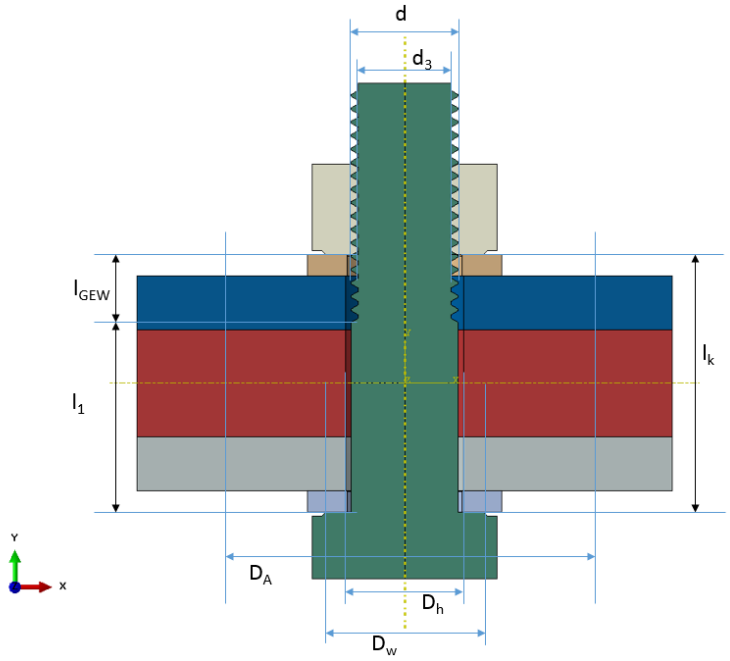

Figure A.1 Dimensions used to estimate resilience of a bolt and clamped plates for calculation of preload loss

Definition of the dimensions and material properties shown in Figure A.1 are listed below:

l_k	*total clamping length*	l_{GEw}	*length of unengaged thread part of the bolt*
l_1	*length of unthreaded bolt shank*	D_w	*effective head diameter*
D_h	*hole diameter*	d	*bolt major diameter*
d_3	*bolt minor diameter*	D_A	*effective diameter of the compressive cone*
A_N	*Major area of the bolt*	A_{d3}	*Minor area of the bolt*

E_s, E_M, E_p *Young's modulus of bolt, nut and plates*

The loss of preload is calculated as $F = \frac{f}{(\delta_s+\delta_p)} = \Delta F_{p,c}$, where f is the contraction (f_y) or embedding (f_z) of the clamped package and δ_s is the elastic resilience of the bolt and δ_p is the elastic resilience of the clamped plates. The total loss of preload due to various factors can be presented as:

$$\Delta F_{p,c} = \Delta F_{p,c,setting} + \cancel{\Delta F_{p,c,relaxation}} + \cancel{\Delta F_{p,c,loosening}} + \Delta F_{p,c,trasnv.\ contraction} + \cancel{\Delta F_{p,c,tenston}}$$

Loss ore preload due to tension, stress relaxation and loosening of the assembly are not considered. For preload loss due to setting and transverse contraction in the slip test, the bolt and clamped plates resilience can be calculated as follows.

Bolt resilience δ_s

The resilience of bolt is calculated as:

$$\delta_s = \delta_{SK} + \delta_1 + \ldots + \delta_{GEW} + \delta_{GM}$$

In which:

$$\delta_{SK} = \frac{0.5 \times d}{E_s \times A_N}; \delta_1 = \frac{l_1}{E_s \times A_N}; \delta_{GEW} = \frac{l_{GEW}}{E_s \times A_N}; \delta_{GM} = \delta_G + \delta_M = \frac{0.5 \times d}{E_s \times A_{d3}} + \frac{0.4 \times d}{E_M \times A_N}$$

Clamped plate resilience δ_p

According to Eqn (5.1/23) in VDI 2331-1, the following applies for the limiting diameter $D_{A,Gr}$ where w = 1 for the through bolted joint,

$$D_{A,Gr} = d_W + l_k \cdot tan(\varphi_D)$$

$$B_L = \frac{l_k}{d_W}$$

It is assumed that the average substitutional outside diameter of the basic solid, allowing for the extent (spacing t) in the circumferential direction up to the next hole wall $D'_A = D_A$. Subsequently:

$$y = \frac{D_A}{d_W}$$

According to Eqn (5.1/27) in VDI 2230-1:

$$tan(\varphi_D) = 0.362 + 0.032 \ln\left(\frac{B_L}{2}\right) + 0.153 \ln y$$

If $D_A \geq D_{A,Gr}$:

$$\delta_p = \frac{2 \ln\left[\frac{(d_w + d_h) \cdot (d_w + w \cdot l_k \cdot \tan(\varphi_D) - d_h)}{(d_w - d_h) \cdot (d_w + w \cdot l_k \cdot \tan(\varphi_D) + d_h)}\right]}{w \cdot E_p \cdot \pi \cdot d_h \cdot \tan(\varphi_D)}$$

If $d_W \leq D_A \leq D_{A,Gr}$:

$$\delta_p = \frac{\frac{2}{w \cdot d_h \cdot \tan(\varphi_D)} \ln\left[\frac{(d_w + d_h) \cdot (D_A - d_h)}{(d_w - d_h) \cdot (D_A + d_h)}\right] + \frac{4}{D_A^2 - d_h^2}\left[l_k - \frac{D_A - d_W}{w \cdot \tan(\varphi_D)}\right]}{E_p \cdot \pi}$$

Transverse contraction f_y

The normal stress over the inner plate can be estimated as:

$$\sigma_x = \frac{F_x}{A} = \frac{F_{s,i}}{A_{gross}} = \frac{n \cdot m \cdot \mu \cdot F_{p,c}}{b_{inner\ plate} \cdot t_{inner\ plate}}$$

Where

$F_{s,i}$ individual slip load

A_{gross} gross cross-section

n number of bolts

m number of plates

μ slip factor

$F_{p,c}$ Preload; $F_{p,c} = 0.7 A_s f_{ub}$

Elastic strain across the thickness of inner plate is then:

$$\epsilon_y = -\frac{v\sigma_x}{E}$$

So that the contraction is

$$f_y = 2\Delta t = 2(\epsilon_y t)$$

Embedment f_z (setting effect)

The amount of embedding primarily depends on the type of working load, the number of interfaces and the magnitude of the roughness of the paired surfaces. Guide values for amounts of embedding are given in Table A.1.

Table A.1 Guide values for amounts of embedding of bolts, nuts and compact clamped parts made of steel

Average roughness height R_Z	Loading	Guide values for amounts of embedding (μm)		
		in the thread	per head or nut bearing area	per inner interface
< 10 μm	tension/compression shear	3 3	2.5 3	1.5 2
10 μm up to 40 μm	tension/compression shear	3 3	3 4.5	2 2.5
40 μm up to 160 μm	tension/compression shear	3 3	4 6.5	3 3.5

APPENDIX B MODEL CALIBRATION OF STAINLESS STEEL PRELOADED CONNECTIONS

Calibration and validation of numerical models of stainless steel slip resistant connections are presented in the following figures. A summary of the validation and comparison of key response parameters are presented in Table 2.7.

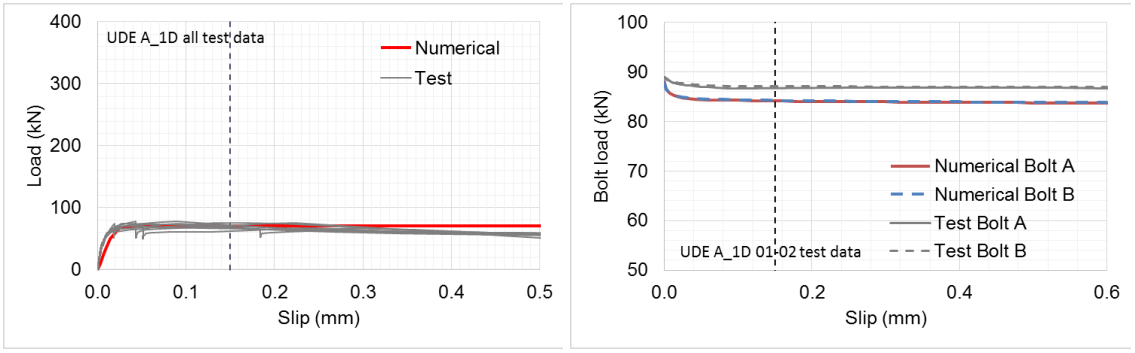

(a) Slip – load curves (b) Loss of preload

Figure B.1 Calibration results for Austenitic plate with as-rolled (1D) surface finish and M16 Bumax 88 bolts (series ID: A_1D)

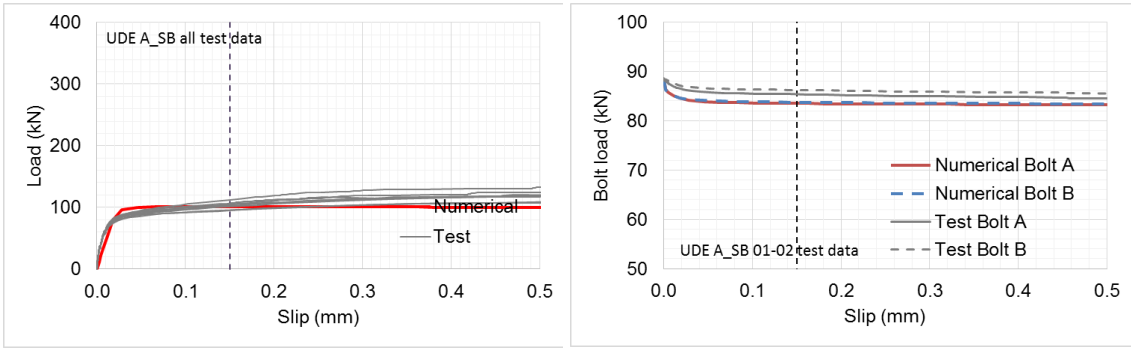

(a) Slip – load curves (b) Loss of preload

Figure B.2 Calibration results for Austenitic plate with shot blasted surface finish and M16 Bumax 88 bolts (series ID: A_SB)

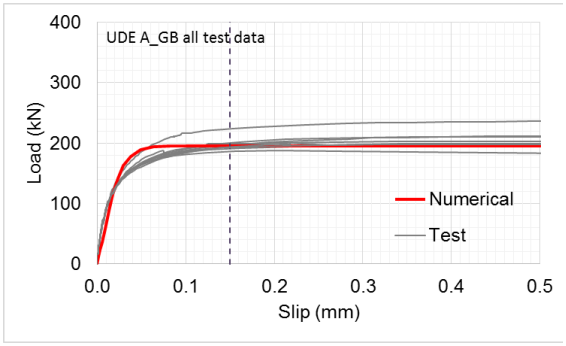

(a) Slip – load curves

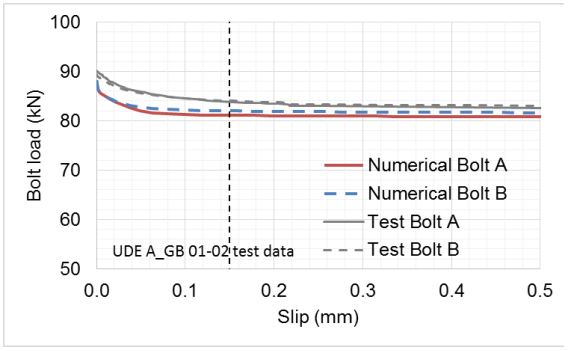

(b) Loss of preload

Figure B.3 Calibration results for Austenitic plate with grit blasted surface finish and M16 Bumax 88 bolts (series ID: A_GB)

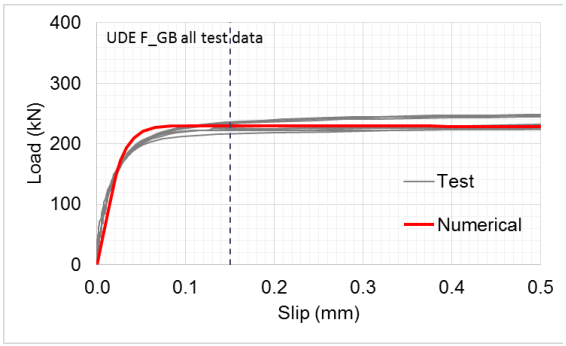

(a) Slip – load curves

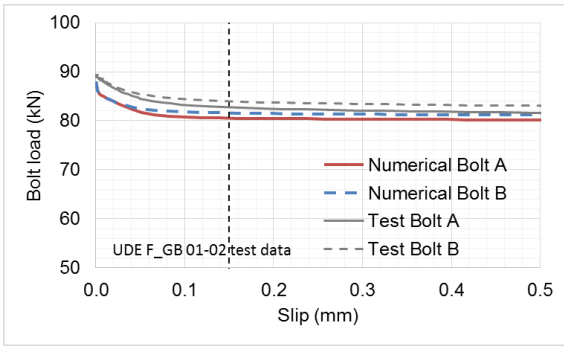

(b) Loss of preload

Figure B.4 Calibration results for Ferritic plate with grit blasted surface finish and M16 Bumax 88 bolts (series ID: F_GB)

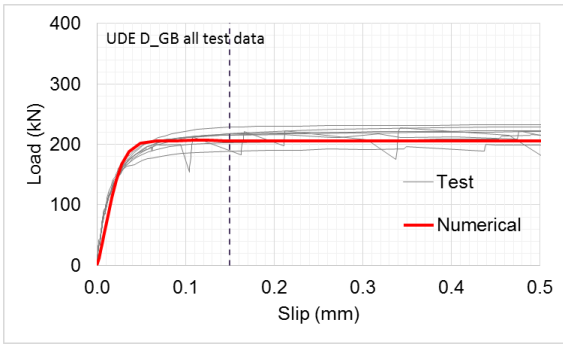

(a) Slip – load curves

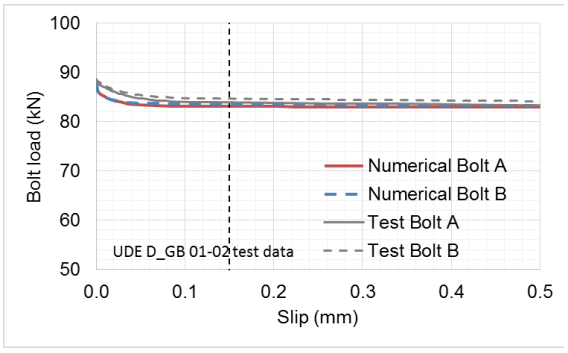

(b) Loss of preload

Figure B.5 Calibration results for Duplex plate with grit blasted surface finish and M16 Bumax 88 bolts (series ID: D_GB)

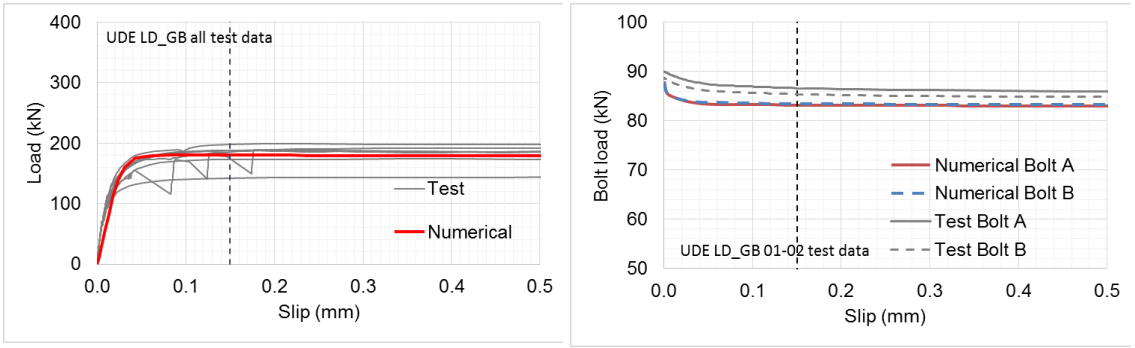

(a) Slip – load curves (b) Loss of preload

Figure B.6 Calibration results for Lean Duplex plate with grit blasted surface finish and M16 Bumax 88 bolts (series ID: LD_GB)

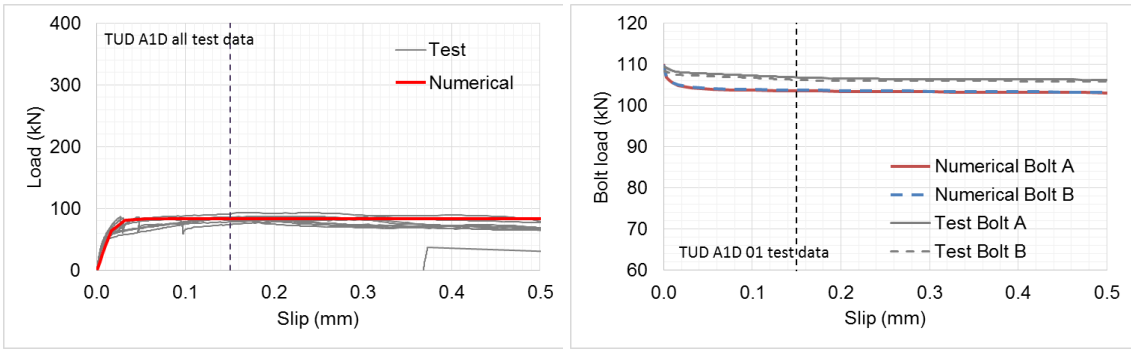

(a) Slip – load curves (b) Loss of preload

Figure B.7 Calibration results for Austenitic plate with as-rolled (1D) surface finish and M16 Bumax 109 bolts (series ID: A1D)

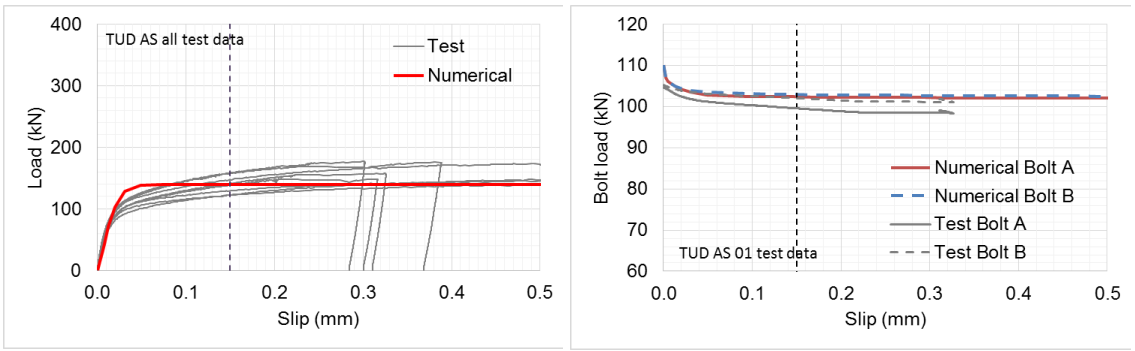

(a) Slip – load curves (b) Loss of preload

Figure B.8 Calibration results for Austenitic plate with shot blasted surface finish and M16 Bumax 109 bolts (series ID: AS)

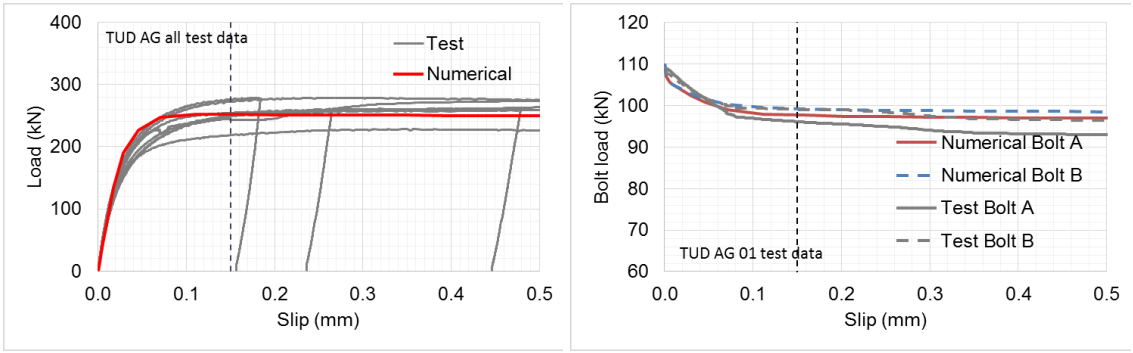

(a) Slip – load curves (b) Loss of preload

Figure B.9 Calibration results for Austenitic plate with grit blasted surface finish and M16 Bumax 109 bolts (series ID: AG)

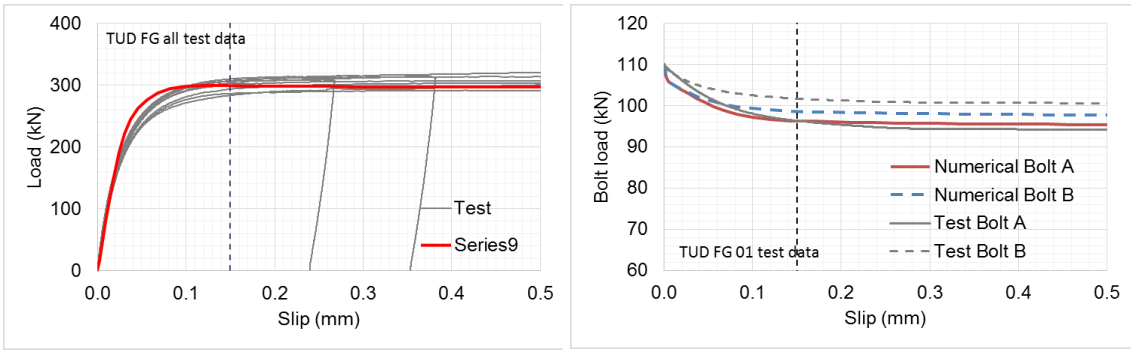

(a) Slip – load curves (b) Loss of preload

Figure B.10 Calibration results for Ferritic plate with grit blasted surface finish and M16 Bumax 109 bolts (series ID: FG)

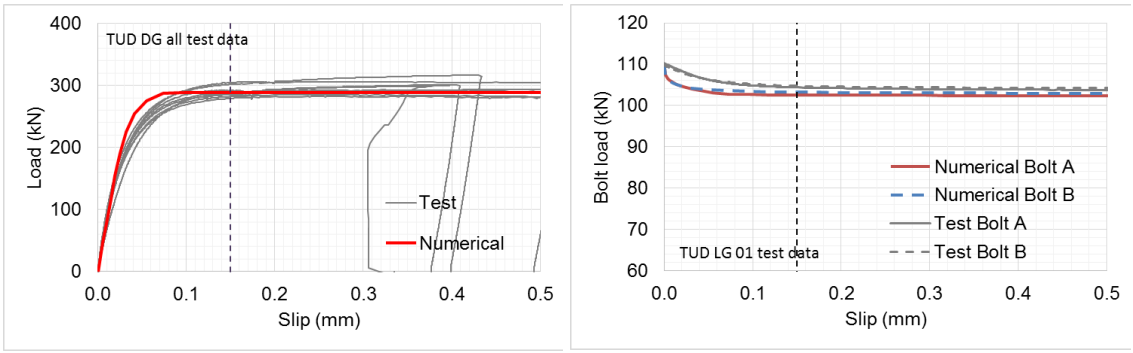

(a) Slip – load curves (b) Loss of preload

Figure B.11 Calibration results for Duplex plate with grit blasted surface finish and M16 Bumax 109 bolts (series ID: DG)

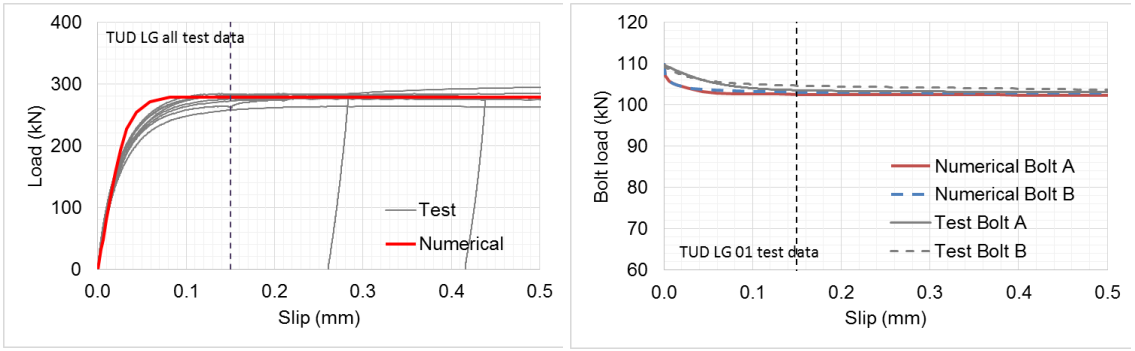

(a) Slip – load curves

(b) Loss of preload

Figure B.12 Calibration results for Lean Duplex plate with grit blasted surface finish and M16 Bumax 109 bolts (series ID: LG)